frontiers | Frontiers in Earth Science

TYPE Review
PUBLISHED 19 April 2023
DOI 10.3389/feart.2023.1139941

OPEN ACCESS

EDITED BY
Venkatramanan Senapathi,
Alagappa University, India

REVIEWED BY
Huan Li,
Central South University, China
Liang Qiu,
China University of Geosciences, China

*CORRESPONDENCE
Yang Song,
songyang100@126.com

RECEIVED 08 January 2023
ACCEPTED 03 April 2023
PUBLISHED 19 April 2023

CITATION
Song Y, Tang J, Lin B, Yang C and Sun H (2023), Metallogeny in the Bangong–Nujiang belt, central Tibet, China: A review.
Front. Earth Sci. 11:1139941.
doi: 10.3389/feart.2023.1139941

Metallogeny in the Bangong–Nujiang belt, central Tibet, China: A review

Yang Song[1]*, Juxing Tang[1], Bin Lin[1,2], Chao Yang[3,4] and Hao Sun[1]

[1]MNR Key Laboratory of Metallogeny and Mineral Assessment, Institute of Mineral Resources, Chinese Academy of Geological Sciences, Beijing, China, [2]Département de Géologie et de Génie Géologique, Université Laval, Québec, QC, Canada, [3]College of Earth Sciences, Chengdu University of Technology, Chengdu, China, [4]London Centre for Ore Deposits and Exploration (LODE), Department of Earth Sciences, Natural History Museum, London, United Kingdom

The Bangong–Nujiang metallogenic belt consists of scattered Tethyan oceanic blocks, mainly distributed underneath the margins of the Qiangtang and Lhasa terranes in central Tibet. A new world-class metallogenic belt has been reported in this region recently, based on the geological mapping and ore deposit prospecting over the last two decades. It currently comprises inferred resources of 30 Mt Cu and 500 t Au, together with several Cr–Ni, Fe, and W (Mo) resources, forming a significant potential area for future mineral exploration. These metals are mainly hosted in porphyry copper, skarn copper, skarn iron, orogenic gold, quartz-vein tungsten, and ophitic chromite deposits. The mineral deposits in the Bangong–Nujiang metallogenic belt have been widely recognized in different localities, including the southern edge of the southern Qiangtang block, part of the north Lhasa block, and even part of the central Lhasa block, indicating they were formed in variable geological settings, from the initial opening, subduction, and collision to the extension of the Bangong–Nujiang Ocean. Specifically, five major tectonic events contributed to mineralization, including the stage 1 (240–165 Ma) initial opening of the Bangong–Nujiang Ocean, stage 2 (165–145 Ma) oceanic subduction, stage 3 (145–100 Ma) close of the ocean, stage 4 (100–65 Ma) continent–continent collisional orogenesis, and stage 5 (65–0 Ma) post-orogenesis. At stage 1, Cr–Ni deposits were formed during the initial opening of the ocean; porphyry–epithermal Cu (Au), skarn Fe, and minor orogenic Au deposits were formed at stage 2 and stage 3; a younger pulse of a few porphyry–skarn Cu ± Mo and orogenic Au deposits were formed during stage 4; finally, W(Mo) deposits were generated in stage 5. In general, porphyry Cu systems, orogenic Au, and skarn Cu polymetallic deposits that occurred in the subduction and post-collision settings related W(Mo) deposits have the most potential for future exploration. An in-depth investigation of several scientific problems, such as addressing the tectonic setting, magmatism, and metallogeny of this region and genetic linkage of these deposit preservations to plateau uplift, is essential for the future success of exploration in the Bangong–Nujiang metallogenic belt.

KEYWORDS

mineral deposits, metallogeny, Bangong–Nujiang, Tibet, China

1 Introduction

The Tethyan orogen is an important metallogenic belt that hosts various types of ore deposits with quantities of metal resources (Richards, 2015; Moritz and Baker, 2019). The eastern part of the Tethyan metallogenic belt, represented by the Tibetan Plateau, has been reported with large amounts of porphyry Cu–Mo–Au, granite-related Sn–W, podiform chromite, sediment-hosted Pb–Zn deposits, volcanogenic massive sulfide Cu–Pb–Zn deposits, epithermal and orogenic Au, as well as skarn Fe, and base metal deposits (Hou and Zhang, 2015), mostly distributed in the Xinansanjiang (Hou et al., 2003; Hou et al., 2007; Liang et al., 2009), Gangdese (Yang et al., 2009; Yang et al., 2014; Yang et al., 2015; Zheng et al., 2016), and Himalaya metallogenic belts (Lin et al., 2016; Tang et al., 2017). The Bangong–Nujiang metallogenic belt (BNMB), located in central Tibet (Figure 1A), is a newly discovered ore deposit cluster with several valuable porphyry Cu–Au deposits that was first reported two decades ago. Its metallogeny has been crudely sketched.

The BNMB has an average elevation of over 4,800 m and is relatively inaccessible by exploration loads due to the impediments of harsh natural environment and poor infrastructure. A few regional geological survey campaigns (larger than 1/250,000 scale mapping) were conducted before 2003, and only a few mineral prospects were found. In recent years, the China Geological Survey (CGS) and the Tibet Geological Exploration Bureau (TGEB) have carried out collaborative geological surveys and mineral resource prospecting projects since 2003 that have contributed to the discovery of many deposits in the BNMB (Figure 1B). Porphyry-skarn copper mineralization is the most important type of ore deposit, mainly including the Duolong ore cluster (Li et al., 2005; Li et al., 2008; Li et al., 2011; Li, 2012; Li et al., 2012; Zhu et al., 2015a; Lin et al., 2017; Song et al., 2018; Lin et al., 2019a), the Ga'erqiong–Galale copper deposits (Zhang et al., 2015a; Wang et al., 2019a), and the Shesuo–Xiongmei copper deposits (Wang et al., 2019b; Wang et al., 2019c; Lin et al., 2022), which are related to the Cretaceous tectonic events of the Bangong–Nujiang suture zone (BNSZ; Zhu et al., 2016; Li et al., 2017a). Therefore, the BNMB is a fertile metallogenetic belt with the potential to yield more mineral resources.

Since 2016, the CGS has implemented a 1:50,000 scale geological mapping project to prospect for copper, gold, iron, lead, zinc, and tungsten deposits in the BNMB. A total area of 33,000 km^2 was mapped between 2016 and 2020, and regional soil and stream geochemistry, trenching, geophysical prospecting, and drilling were integrated for the metal resource survey. Quantities of new

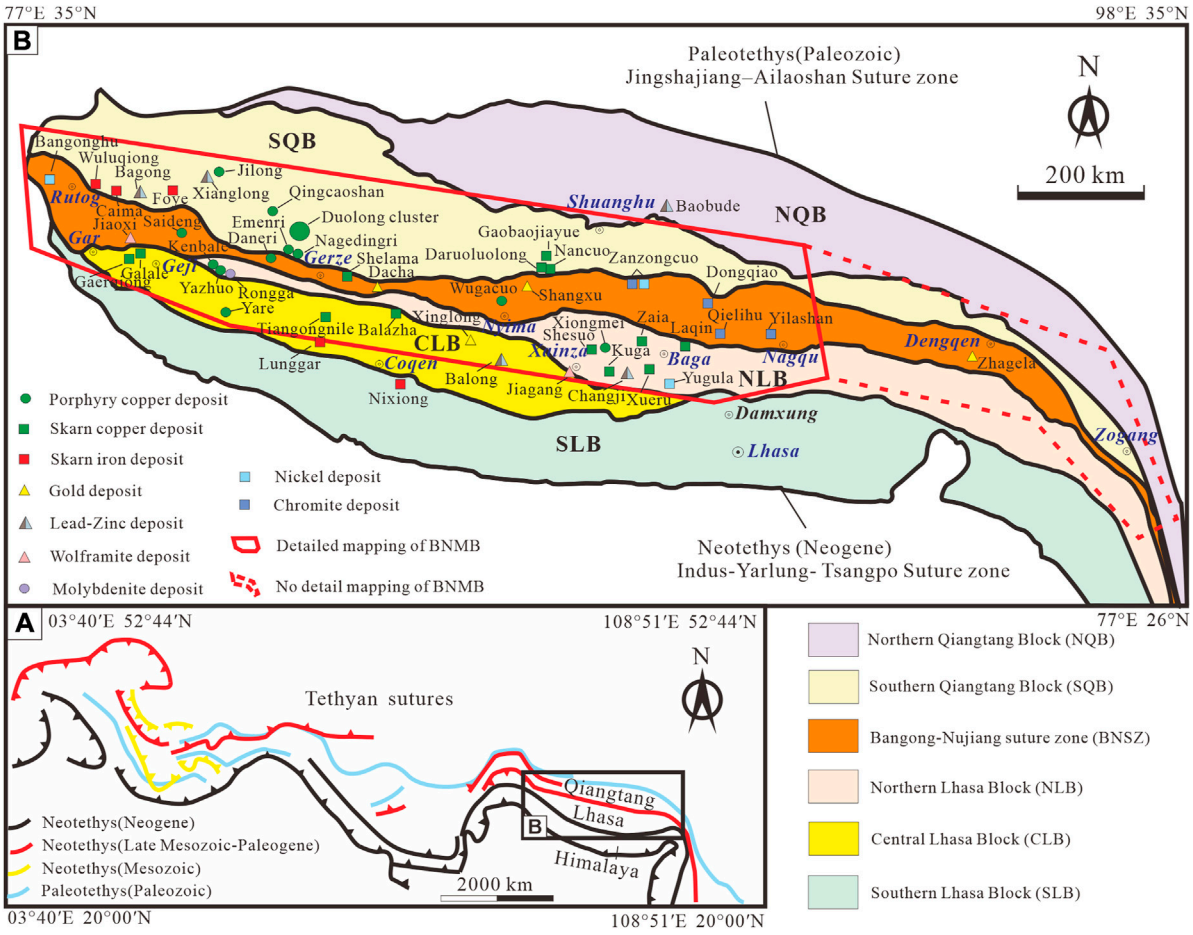

FIGURE 1
(A) Framework of the Tethyan suture zone. **(B)** Tectonic units and ore deposits in the Bangong–Nujiang metallogenic belt.

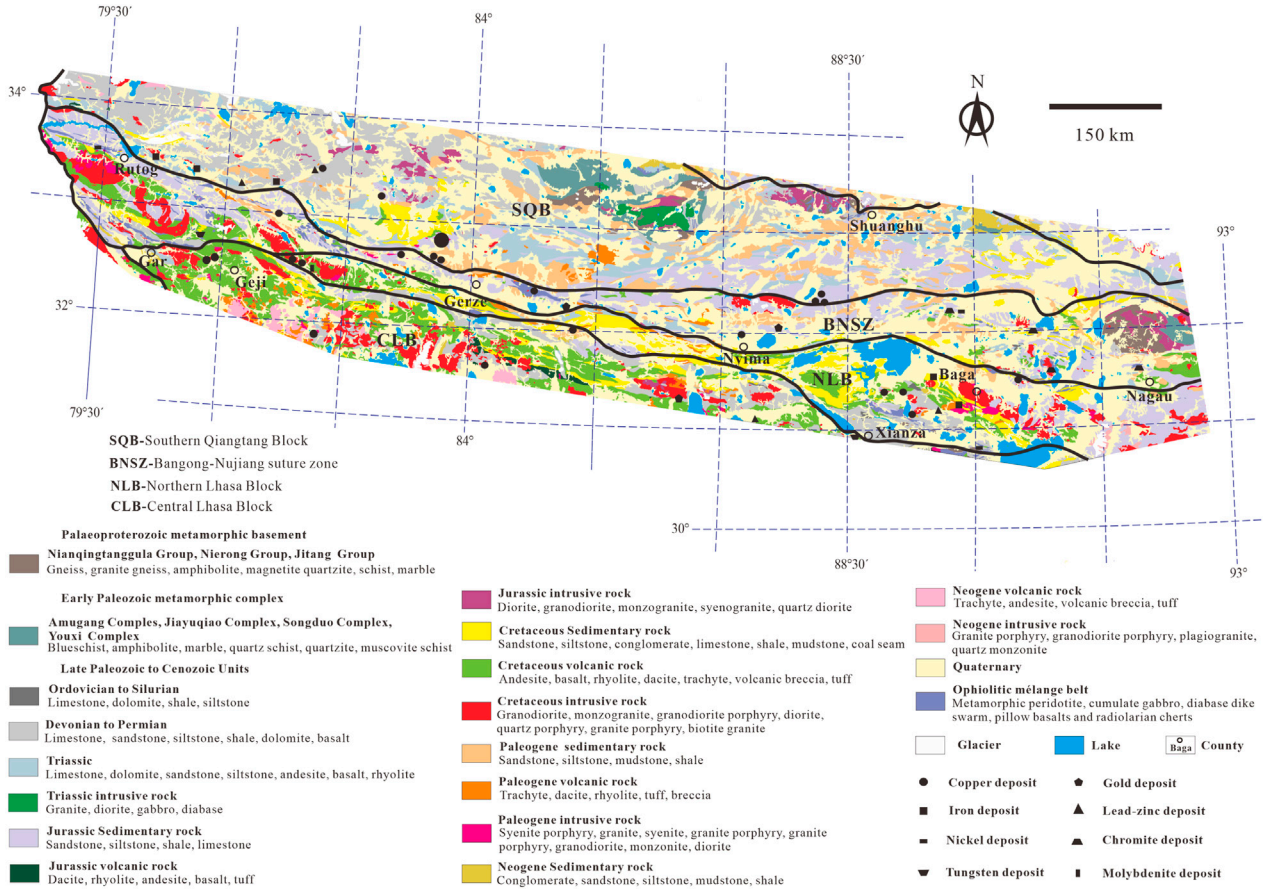

FIGURE 2
Geology of the Bangong–Nujiang metallogenic belt.

deposits were discovered during the survey. A comprehensive review of the mineral deposits and geological evolution of the BNMB may help to understand the metallogeny of this belt and aid future exploration.

This paper will review the geology and various mineral deposits of the BNMB based on recently published literature and the CGS reports, which cover 57 documented ore deposits, prospects, and occurrences, with detailed information listed in the Supplementary Material (Supplementary Table S1). We further demonstrate the regional geological framework of these ore deposits in terms of their host petrology units, deposit types, and geochronology, and propose their genetical relationship to the history of the Tibetan plateau uplifting. Finally, we discuss the implications for copper, gold, tungsten, and molybdenum exploration and propose an outlook for future investigations in the BNMB.

2 Regional geology

The BNSZ separates the Qiangtang block from the Lhasa block (Yin and Harrison, 2000). The Qiangtang block is bounded by the Jinsha suture to the north and the Bangong–Nujiang suture to the south, and the Lhasa block lies between the Indus–Yalu and Bangong–Nujiang sutures (Yin and Harrison, 2000). Based on the different rock units, the Qiangtang block is roughly divided into the northern and the southern subblocks bounded by the Longmu–Shuanghu suture (Pan et al., 2012), while the Lhasa block can be divided into northern, central, and southern subblocks, bounded by the Shiquan River–Nam Tso Mélange Zone (SNMZ) and the Luobadui–Milashan Fault (LMF), respectively (Zhu et al., 2011). The BNMB is defined by ore deposits distributed not only in the BNSZ, but also in the magmatic arcs of the southern Qiangtang block (SQB) to the north and the north Lhasa block (NLB) and central Lhasa block (CLB) to the south (Figure 1B; Li et al., 2009). The BNSZ is the boundary between the Qiangtang and Lhasa terranes, extending >2000 km across the central Tibetan Plateau from Bangong Co in the west, through Gaize, Nyima, Dongqiao, Amdo, and Dengqen (Figure 1B) in the east, and then turning to the south to the Nujiang River (Pan et al., 2006). It is characterized by scattered ophiolite fragments consisting of thick sequences of Jurassic flysch, mélange, and volcanic rocks (Kapp et al., 2003).

2.1 Stratigraphy

The strata of the BNMB are subordinate to the Dian (Yunnan)–Tibet stratigraphic dome, from north to south, including the

southern Qiangtang stratigraphic region, the Bangong–Nujiang stratigraphic region, and the northern Gangdese stratigraphic region (Figure 2). The southern Qiangtang stratigraphic region can be further divided into the Qiangnan strata (southern part of Qiangtang) and the Zuogong strata (eastern Tibet) (Song et al., 2014). The Zuogong strata consist of Bangong–Nujiang ophiolitic mélange zone, the Nyainrong microcontinent, and Jiayuqiao metamorphic complex. The Baga–Xainza strata and the Geji–Coqen strata constitute the northern Gangdese stratigraphic zone (Figure 2; Song et al., 2014).

The oldest stratum of the BNMB is the Palaeoproterozoic basement, characterized by metamorphic rocks of the Nianqingtanggula, Nierong, and Jitang groups, which comprise gneiss, granite gneiss, amphibolite, magnetite quartzite, schist, and marble. The basement is presented in the eastern parts of the belt; sporadic outcrops also occur in the northern part of the SQB (Figure 2). The metamorphic complex formed in the Early Paleozoic rocks, including Amugang, Jiayuqiao, Songduo, and Youxi complexes, with blueschist, amphibolite, marble, quartz schist, quartzite, and muscovite schist. They are mainly distributed near the metamorphic basement (Figure 2). Paleozoic to Cenozoic units are widespread in the whole belt. They contain Ordovician to Neogene sedimentary rocks. The main lithology types are limestone, dolomite, shale, siltstone, sandstone, mudstone, conglomerate, and coalseam. Among them, the Ordovician to Silurian sedimentary rocks of the Early Paleozoic are confined to the Baga–Xinza area, and the Late Paleozoic Devonian to Permian sedimentary rocks are widely distributed in the western part of the SQB within the belt or occur in the discontinuous bands in the southern part of the belt (Figure 2). Triassic to Cretaceous sedimentary rocks are broadly distributed in the entire belt. Triassic strata are mainly presented in the northern part of the BNSZ in an east–west direction. Jurassic sedimentary rocks are widely developed, generally passing through the belt from the west to the east, and are also distributed in a large area in the southeast corner of the belt. The main body of Cretaceous sedimentary rocks is distributed along the direction of the BNSZ in the southern part of the belt (Figure 2). Paleogene and Neogene sedimentary rocks are mainly distributed in the north of the Lhasa block within the belt (Figure 2).

Jurassic strata have been unconformably overlain by Middle–Upper Triassic strata, indicating that the Bangong–Nujiang Ocean (BNO) was reactivated, and the newly formed Pangea continent dissociated in Tibet (Pan et al., 2012). Paleogeographic sedimentary features, such as a deep the sea basin, ophiolitic oceanic crust, continental shelf, and coastal environment, appeared in the SQB, BNSZ, and NLB. The prologue of the BNSZ dissociation began at the Middle Triassic and had been pulled into the ocean by the end of the Late Triassic. The Jurassic paleogeographical setting is characterized by remnant ocean, arc, deep sea, and residual sea, representing the BNO reduction (Song et al., 2019a). The late Cretaceous molasse and related volcanic rocks are evidence of orogenic events and tectonic uplift at that time (Kapp et al., 2007; Liu et al., 2018; Lai et al., 2019).

The southern Qiangtang stratigraphic region and the northern Gangdese stratigraphic region have the same sedimentary strata in the Late Paleozoic–Early Mesozoic, suggesting they were formed in the same sedimentary environment before it was separated by the opening of the BNO (Song et al., 2019a). The Longmuco–Shuanghu–Jinjiang suture zone was formed from the Late Devonian to the end of the Late Triassic, possibly to the Early Paleozoic, which was considered to represent the boundary between the Gondwana and Yangtze plates during the Carboniferous and Permian periods (Li et al., 2009; Lv et al., 2011; Liang et al., 2017). Therefore, the corresponding sedimentary system, including the Paleo-Tethys Basin, continental margin, and accretionary material, was deposited (Zhang et al., 2013; Zhang et al., 2017).

2.2 Magmatism

Intrusive rocks of the belt mainly emplaced in the Mesozoic and Cenozoic, while Paleozoic intrusive rocks were scarce. Intrusive rock types mainly consists of granite, diorite, gabbro, diabase, granodiorite, monzogranite, granodiorite porphyry, quartz porphyry, granite porphyry, biotite granite, syenite porphyry, syenite, monzonite, granite porphyry, plagiogranite, quartz monzonite, and quartz diorite. Triassic intrusive rocks are confined to the northern part of the belt (Figure 2).

Late Jurassic–Early Cretaceous magmatism is widespread in central Tibet, occurring along the southern margin of the SQB, as well as in the central and western sections of the Lhasa block (Figure 2). There are mainly three phases of magmatism. Phase 1 (140–130 Ma) was suggested to be associated with the flat subduction of the Bangong–Nujiang oceanic slab (Li et al., 2018) and arc-arc "soft" collision (Zhu et al., 2016). Phase 2 magmatism (120–110 Ma) occurred on both sides of the BNSZ, which was reactivated by the sinking and breakoff of the Bangong Tethyan Ocean lithosphere (Zhu et al., 2016; Li et al., 2018; Lin et al., 2019a). A wide range of volcanic rocks also erupted during phase 2 magmatism, including the Meiriqiecuo, Qushenla, and Duoba (or Duoni) formations (Song et al., 2019a). The youngest magmatic episode is emplaced at the Late Cretaceous (ca. 90 Ma), mainly distributed in the NLB (Wang et al., 2019a; Lei et al., 2019). Additional magmatic events, including Cenozoic intrusive and volcanic rocks at various times (ca. 65–15 Ma), are mainly distributed along the CLB (Figure 2), which records the geodynamic setting changes that are related to the India–Asia collision (Mo et al., 2003; Mo et al., 2008; Wang et al., 2015; Hou et al., 2020).

Mesozoic and Cenozoic volcanic rocks dominate the belt, while Paleozoic volcanic rocks are less common, which is consistent with the intrusive rocks. Mesozoic volcanic rocks mainly include Jurassic dacite, rhyolite, andesite, basalt, and tuff, and Cretaceous rocks include andesite, basalt, rhyolite, dacite, trachyte, volcanic breccia, and tuff. Jurassic volcanic rocks occur only in small quantities in the southern part of the belt, while Cretaceous volcanic rocks, the most abundant volcanic rock in the belt, prevail in the southern part of the entire belt (Figure 2).

2.3 Hosts of different mineralization types

At present, 57 deposits, prospects, and occurrences were reported in the BNMB. The deposit types include porphyry copper, skarn copper, skarn iron, orogenic gold, quartz-vein

10.3389/feart.2023.1139941

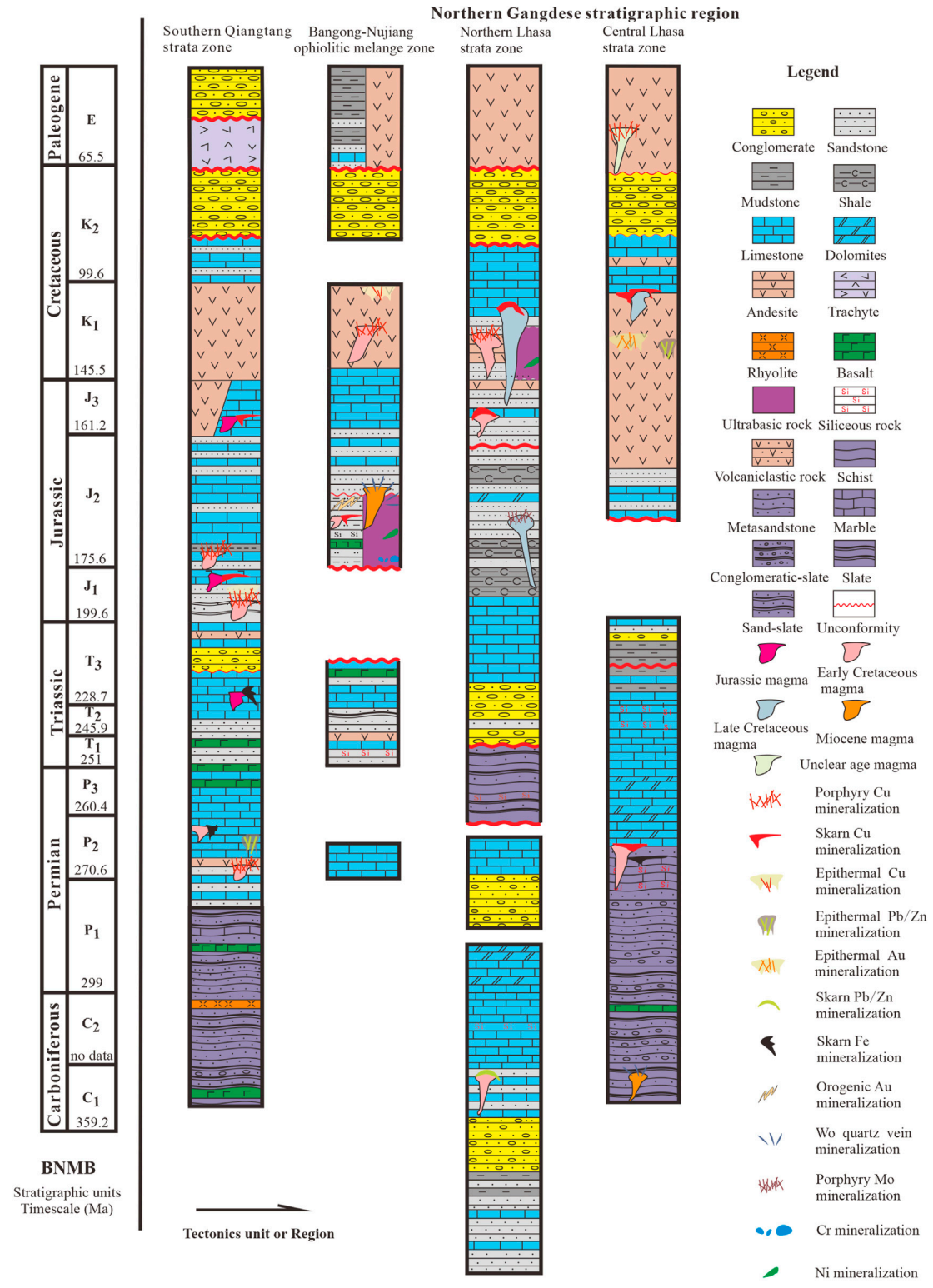

FIGURE 3
Sketch of host strata, intrusion, and ore deposit relationships in the Bangong–Nujiang metallogenic belt.

tungsten, and ophitic chromite deposits. The Early Cretaceous porphyry deposits are mainly hosted in the Jurassic sedimentary rocks in the SQB (Figures 3). The sedimentary rocks consist of conglomerate, sandstone, metamorphic siltstone, and slate (Figure 3). The Early Cretaceous andesite in the Duolong district is recognized as post-ore cover that protects the ore deposits, such as

the Tiegelongnan deposit, from erosion (Lin et al., 2017; Song et al., 2017; Tang et al., 2017; Song et al., 2018; Lin et al., 2019b; Yang et al., 2020a; Yang et al., 2020b). The Early Cretaceous andesite in the central BNSZ and NLB hosts several porphyry deposits, such as the Wugacuo and Saideng deposits (Wang et al., 2017a; Wang et al., 2017b; CGS report). Lower Cretaceous argillaceous siltstone is the main host rock type of Xiongmei. The skarn deposits in the SQB are hosted in the limestone of the Permian, Triassic, and Jurassic (Figure 3). In the Baga–Xainza zone, skarn deposits are hosted in limestone, shale, and volcaniclastic rocks of the Carboniferous, Jurassic, and Cretaceous. Skarn ores are commonly presented along the contact between the intrusive rocks and limestone, such as the Ga'erqiong and Galale deposits (Figure 3; Zhang et al., 2015a; Wang et al., 2019a). Some skarn iron deposits occur in the Permian conglomerate and slate and in the Xiala metasandstone in the Geji–Coqen area. Orogenic Au-bearing lodes occur in the sandstone and sand slates (Figure 3). Ores hosted in the metamorphic graywacke, mudstone, and carbonaceous slate feature low-green schist facies metamorphism in Shangxu. Wusuola (or Dacha) and Zhagela gold deposits are hosted in the Jurassic metamorphic flysch rocks. The Cr-Ni deposits are mainly hosted in the ultramafic part of the ophiolite complex (Figure 3). For example, the Dongqiao chromite deposit contains dunite and harzburgite, which mainly host a 130 massive, disseminated, nodular, and podiform chromite ore bodies (length>20 m, 12%) and lesser amounts of basaltic lava and basic–ultrabasic cumulate. The Yugula nickel deposit is situated within the ultramafic rock of the ophiolite suite at the southern margin of the NLB. The quartz-vein W deposit, Jiagang (or Gariatong), is with the Carboniferous limestone and slate strata of the Yongzhu Group (Figure 3) (Lin et al., under review); the Jiaoxi W deposit is hosted in Miocene porphyritic monzogranite, sandstone, and shale, forming the quartz–muscovite–wolframite veins (Wang et al., 2018a).

3 Ore deposit types

Most of the deposits investigated in this study are in a preliminary exploration level, and their resources are still under investigation. Detailed information in terms of deposit mineralogy, structure, size, age, and stratigraphic and tectonic settings of these deposits are summarized in Supplementary Table S1**.** The details of different deposit types are discussed in the following sections.

3.1 Porphyry copper deposits

Porphyry Cu deposit is the main ore type in the BNMB, accompanied with some epithermal ore bodies, as part of the porphyry copper system (Ballhaus, 1998). The porphyry copper deposits are mostly found in the South Qiangtang block (Figures 1, 2), represented by the Qingcaoshan, Jilong, and Duolong ore clusters. Some porphyry deposits are presented in the BNSZ, such as the Saideng, Daneri, and Wugacuo deposits, and some are in the Lasha block, including the Kenbale and Yazhuo and Yare and Xiongmei deposits (Figure 1). Copper is the dominant metal from these porphyry deposits, with Au, Ag, and Mo as secondary metals in some deposits. In terms of tonnage of Cu metal, there is one giant deposit (>10 Mt Cu, Tiegelongnan), four large porphyry deposits (>1 Mt and <10 Mt Cu, e.g., Bolong, Duobuza, Nating, and Naruo), four intermediate deposits (>0.1 Mt and <1 Mt Cu, e.g., Yare, Saideng, Emenri, and Qingcaoshan), and 12 small deposits (<0.1 Mt Cu, e.g., Xiongmei, Gaerqin). Most of those large deposits have a low Cu grade of less than 0.5%, but the giant Tiegelongnan deposit has a relatively high grade of 0.53% Cu (Figure 4A). Several intermediate deposits (e.g., the Saideng and Emenri) and small deposits (e.g., Nagedingri and Daneri) have high Cu grades of over 1% (Figure 4A). Some also contain significant amounts of gold, such as the Tiegelongnan, Bolong, Nating, Naruo, and Duobuza deposits, with over 60 tons Au at a relatively low grade of around 0.2 g/t (Figure 4B). Silver commonly occurs in these Au-bearing porphyry deposits. The BNMB is not a major source of molybdenum, except that Rongga contains 11,940 t @ 0.091% Mo (Qu and Xin, 2006; Qu et al., 2009; Qu et al., 2012; Qu, 2016; Qiao et al., 2017; Peng et al., 2019). The Yare deposit was reported to have 14,600 t Mo; however, an Mo grade was not included in the CGS report. In addition, several porphyry and epithermal base metal deposits occur in the BNMB, such as the Bagong, Xianglong, Balong, Baobude, and Yare deposits, which host Pb and Zn resources.

These large-to-giant porphyry Cu (Au, Ag) deposits (e.g., Tiegelongnan, Bolong, Nating, Duobuza, and Naruo) are located in the Duolong ore cluster (Figure 5), within the SQB. The Duolong area is approximately 50 km long and 18 km wide and is one of the biggest porphyry Cu regions in China. In addition to the five major porphyry deposits, it also hosts three small deposits, namely, Gaerqin, Sena, and Nadun, and several porphyry prospects (Figure 5; Li et al., 2017a; Zhu et al., 2015c; Lin et al., 2019b). These porphyry deposits in the BNMB are associated with Cretaceous porphyries. Granodiorite and diorite porphyries, found in the Xiongmei, Duobuza, Bolong, Naruo, and Tiegelongnan deposits, are the major intrusions related to Cu-Au mineralization. Monzonite porphyry, found in Rongga, is associated with Mo mineralization. Yazhuo is related to diorite porphyry. The related intrusions of some deposits, such as Emenri, have not yet been found, but they have porphyry-type alteration and veins. Thus, these deposits are also referred to as porphyry deposits.

Each porphyry deposit exhibits a different degree of hydrothermal alteration. Even in one district, such as Duolong, the major ore stage occurs in different alteration zones between different deposits. For example, Duobuza and Bolong deposits are mainly associated with potassic alteration (Zhu et al., 2012; Zhang et al., 2015c), whereas the advanced argillic and phyllic alterations host high-grade ores at Tiegelongnan, and ores are hosted in propylitic alteration in the Nating deposit. In general, potassic, phyllic, and propylitic alterations are common types in those deposits, with some argillic overprinting and carbonation. The Tiegelongnan, Nadun, and Dibaonamugang deposits are the only three deposits with advanced argillic alteration that host high-sulfidation epithermal mineralization (Tang et al., 2014a; Tang et al., 2014b; Tang et al., 2016; Song et al., 2018; Yang et al., 2020a; Yang et al., 2020c). Nagedingri also has kaolinite alteration; however, its genesis is not clear. Chalcopyrite is the principal copper sulfide, with a few deposits having bornite as subsidiary copper carrier. Supergene Cu-sulfides including covellite, digenite, and chalcocite, and Cu-oxides, such as

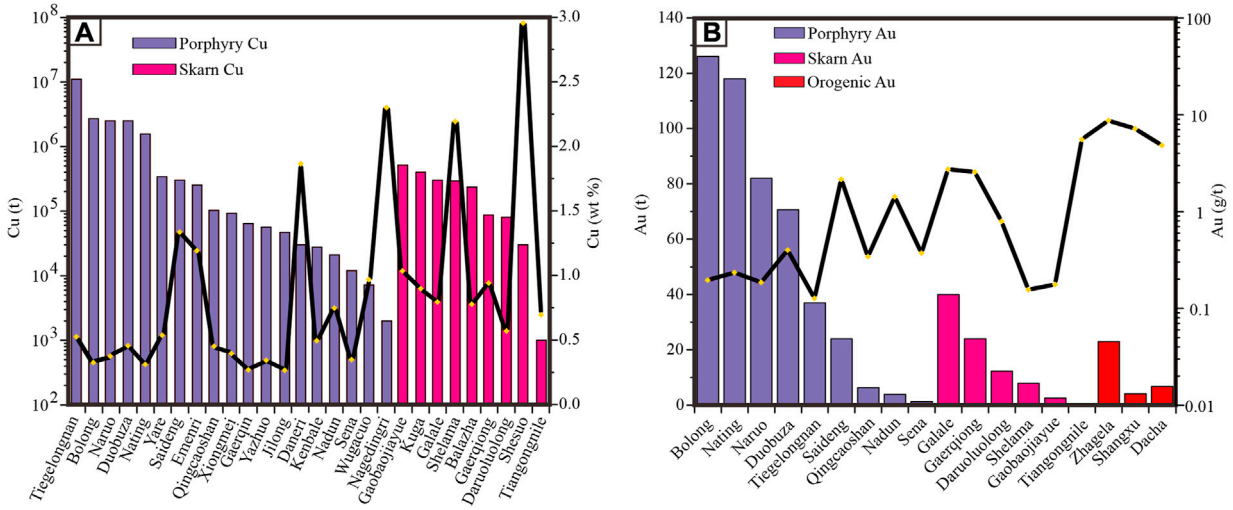

FIGURE 4
(A) Copper, **(B)** gold resources, and grade of the major deposit types in the Bangong–Nujiang metallogenic belt.

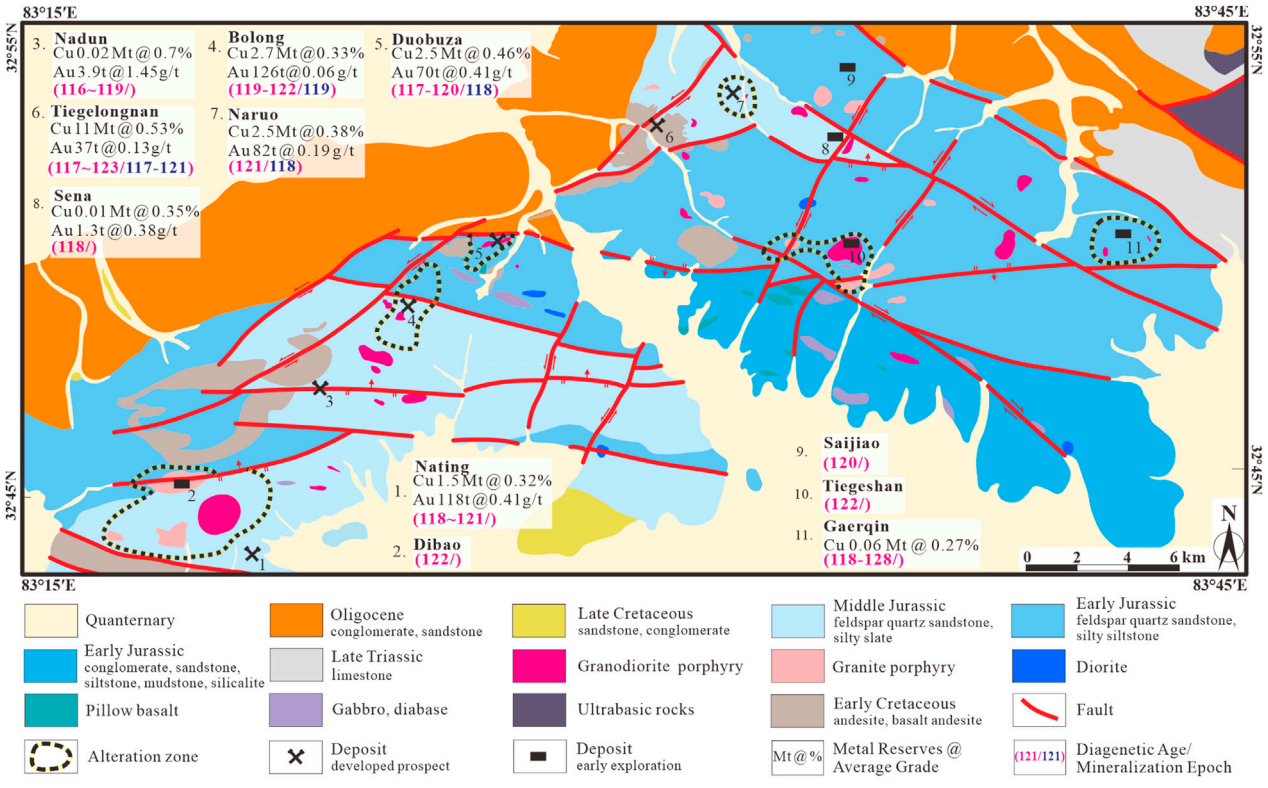

FIGURE 5
Geology and location of porphyry Cu and Au deposits in Duolong District (modified from Lin et al., 2017).

malachite and lazurite, are presented in some deposits. Hypogene high-sulfidation minerals digenite, covellite, enargite, and tennantite are also found in several deposits, such as Tiegelongnan and Nadun deposits.

3.2 Skarn copper and iron deposits

Skarn-type copper and iron mineralization is another important type of deposit in the BNMB. Copper resources dominate nine of

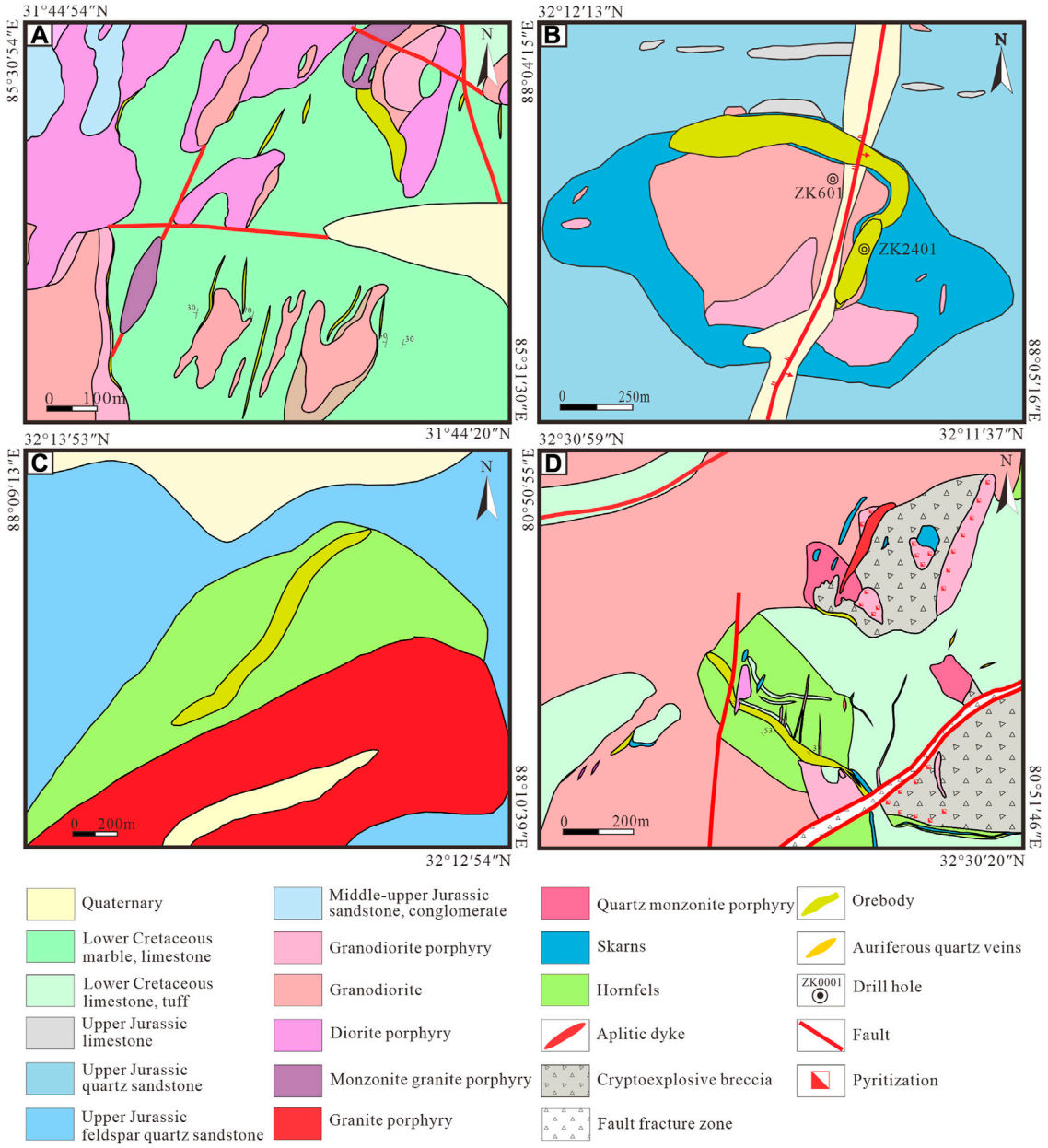

FIGURE 6
Geology of skarn deposits. **(A)** Balazha deposit (modified from Wang et al., 2013), **(B)** Daruoluolong deposit (modified from Wang et al., 2019d), **(C)** Gaobaojiayue deposit (modified from No. 5 Geological Party, Tibet Bureau of Geology and Exploration of Mineral Resources, 2014), and **(D)** Ga'erqiong deposit (modified from Tibet Institute of Geological Survey, 2009).

fourteen reported skarn deposits, five of which including Gaobaojiayue, Kuga, Galale, Shelama, and Balazha, contain more than 0.1 Mt of Cu individually. The copper grade of skarn deposits is generally higher than porphyry copper deposits and reaches 2.96% in the Shesuo deposit (Figure 4A). Some skarn copper deposits are also associated with gold mineralization, such as the Galale, Ga'erqiong, and Shelama. (Figure 4B). The Galale and Ga'erqiong deposits have high Au grades at 2.8 g/t and 2.61 g/t, respectively. Iron is also valuable metal resource in several skarn deposits, and it has been the primary exploration target in the BNMB. The skarn Fe deposits include the Nixiong and Lunggar Fe deposits in the CLB and SLB with 150 Mt (55%–66% Fe_2O_3T) and 37 Mt (56% Fe_2O_3T) ores, respectively, and the Caima and Fuye deposits in the SQB with 11.5 Mt (43%–68%, Fe_2O_3T) and 9.1 Mt (57%–63%, Fe_2O_3T) ores, respectively. The Changji deposit is a recently discovered skarn Pb–Zn–Ag deposit, with 562,000 t @ 2.68% Zn, 105,000t @ 0.3% Pb, and 600 t @ 20 g/t Ag (Song et al., 2022). Wang et al. (2012b) and Ding et al. (2012) reported that Zaia and Xueru are small skarn Fe deposits that occur in the contact zone between the granodiorite (80 Ma) and the Lower Cretaceous Langshan limestone, but the amount of the resource remains unclear. Zhanting, Meihuashan, Congbari, Pianqu, Bangai, and Wuluqiong prospects were formed in

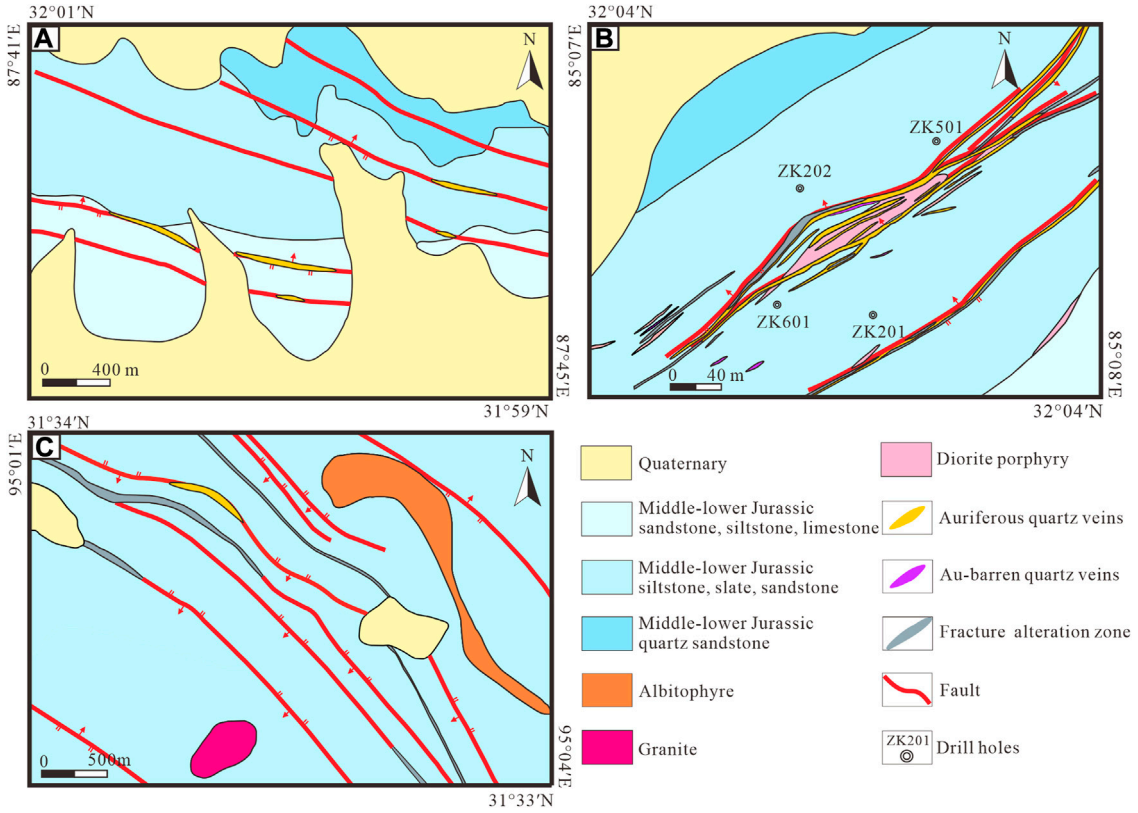

FIGURE 7
Geology of orogenic gold deposits. **(A)** Shangxu deposit (modified from Huang et al., 2014), **(B)** Dacha (Wusuola) deposit (modified from Tibet Institute of Geological Survey, 2010), and **(C)** Zhagela deposit (modified from Zhang et al., 2015b).

the contact zone between the intermediate-felsic intrusive rocks (161–157 Ma) and carbonate rocks (Yang et al., 2018).

Porphyritic intrusions are found in most of those skarn deposits and mostly are granodiorite, diorite, and monzonite (Figure 6). Alteration of these skarn Cu deposits has not yet been clearly documented. Sulfides in skarn Cu deposits consist of mainly pyrite and chalcopyrite and minor amounts of bornite, sphalerite, molybdenite, and pyrrhotite. Supergene covellite, chalcocite, and the Cu-oxides azurite and malachite were found in some deposits. Magnetite and hematite are the major iron sources for skarn iron deposits, which also contain small numbers of sulfides, such as chalcopyrite, pyrite, bornite, galena, and pyrrhotite.

3.3 Orogenic gold deposits

Three orogenic gold deposits were reported in the BNMB, including the Dacha (or Wusuola) (6.73 t @ 3.54 g/t Au), Shangxu (4.12 tons @ 7.36 g/t Au), and Zhagela deposits (23 tons @ 8.9 g/t Au). They are located in the suture zone from the western to eastern parts of the central BNSZ (Figures 1, 2). Although these orogenic Au deposits provide smaller amounts of Au resources than porphyry and skarn Au deposits in total, they have relatively high grades at 6–10 g/t (Figure 4B).

These deposits are mainly hosted by middle-lower Jurassic sedimentary rocks, and gold occurs in quartz veins (Figure 7). Hydrothermal alteration minerals associated with Au mineralization are characterized by muscovite, carbonate, sulfide, and chlorite. Sulfide minerals include pyrite, chalcopyrite, sphalerite, galena, and marcasite, with minor amounts of arsenopyrite, pyrrhotite, tetrahedrite, digenite, bornite, millerite, gersdorffite, and cobaltite (Fang et al., 2020a; Fang et al., 2020b). Drill hole logging revealed massive-to-laminated quartz veins, spur, saddle reef, and disseminated ore. Native gold usually occurs in these quartz veins.

3.4 Ophiolite-related chromite and nickel deposits

The chromium and nickel resources in the BNMB have been explored and mined in the Dongqiao and Qielihu deposits since the 1950s. Currently, there are five Cr and Ni deposits being reported with metal resources, and the Zanzongcuo is a new discovery. Most of the Cr and Ni deposits are distributed in the BNSZ and are related to ophiolites, except the Yugula deposit (Figures 1, 2). The Dongqiao, Qielihu, and Yilashan are Cr deposits; a few nickel sulfides are also reported in the Dongqiao and Qielihu deposits. The Bangonghu and Yugula

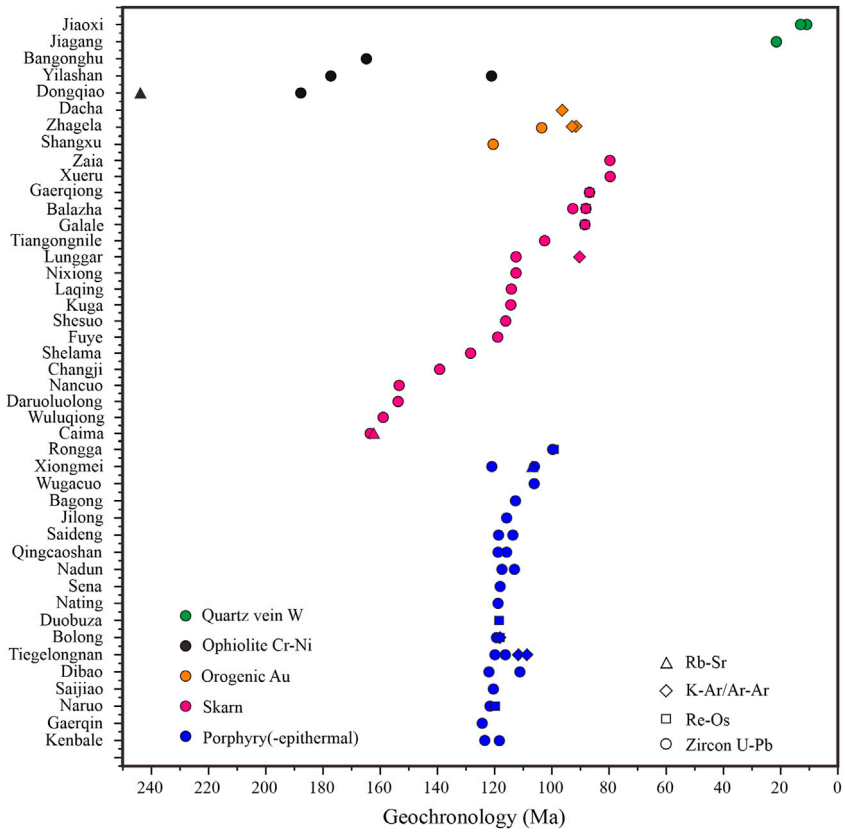

FIGURE 8
Geochronology of ore deposits in the Bangong–Nujiang metallogenic belt.

are Ni deposits, and Zangzongcuo is a Cr–Ni deposit. Podiform chromite is the major Cr carrier. Disseminated millerite, which coexists with magnetite, is the primary Ni sulfide, constituting the layered and strip-shaped ore bodies.

3.5 Quartz-vein tungsten (molybdenite) deposits

Two tungsten deposits, the Jiagang (18,900 tons @ 1.12% WO_3) and the Jiaoxi (39,100 t @ 1.12% WO_3), have been found in the BNMB recently. The Jiagang deposit is hosted in the Lhasa block, and the Jiaoxi deposit is in the western BNSZ (Figures 1, 2). The Jiagang W–Mo deposit is a quartz-vein wolframite deposit with greisen alteration (Ge et al., 2004; Wang et al., 2006a; Wang et al., 2006b). However, Xu et al. (2017) and Xu et al. (2020) believe that the Jiagang deposit is a greisen-type tungsten deposit, based on widely developed greisen alteration and the occurrence characteristics of ore veins. The Jiaoxi W deposit is a typical quartz-vein type tungsten deposit (Wang et al., 2018b; Wang et al., 2018c; Wang et al., 2019e). The wolframite-bearing quartz veins are hosted in the monzonitic granite and surrounding country rocks of both of these deposits. The quartz veins also contain a small amount of molybdenite and bismuthinite. Quartz and white mica are the typical hydrothermal alteration assemblage.

4 Metallogeny

4.1 Geochronology

Porphyry Cu deposits in the BNMB were formed during the Early Cretaceous (125–100 Ma), mostly at 120–115 Ma (Figure 8). The timing of porphyry deposits is mostly constrained by the zircon U-Pb ages of the related intrusions. In a few deposits, multiple stages of porphyries are distinguished with different ages, such as the Xiongmei, Saideng, Qingcaoshan, Dibao, and Nadun. However, the relationships between mineralization and intrusions are unclear. Thus, several analytical methods were used to confirm the magmatism and hydrothermal events of some well-constrained deposits. For example, both molybdenite Re–Os ages and alteration mineral (K-feldspar and biotite) Ar–Ar ages obtained from the Duobuza, Bolong, and Tiegelongnan deposits have been applied to confirm that the hydrothermal ages are consistent with the ages of granodiorite and diorite porphyries (Zhu et al., 2015a; Zhu et al., 2015b; Ding et al., 2017; Lin et al., 2018a). Zircon U–Pb and whole-rock Rb–Sr isochronal age show Xiongmei Cu-bearing granodiorite porphyry formed during 110–105 Ma (Xiao et al., 2017; Wang et al., 2019c). The detailed geochronology in the Tiegelongnan deposit shows that at least three porphyry and epithermal hydrothermal events at 120 Ma, 116 Ma, and 112 Ma contributed to this giant Cu deposit (Yu et al., 2011a; Yu et al., 2011b; Yu et al., 2012; Yang et al., 2020a).

Ages of skarn deposits are more widely spread than porphyry deposits, from the Middle Jurassic to the Late Cretaceous (Figure 8). The oldest Caima skarn Fe deposit formed at ca. 165 Ma, constrained by the zircon U-Pb age and the whole-rock Rb–Sr age of the monzonite granite (Zhao et al., 2009; Zhao et al., 2011; Zhang et al., 2011; Zheng et al., 2021; Zhou et al., 2013). However, the youngest Zaia and Xueru deposits are associated with porphyries formed at 79 Ma (Wang et al., 2012a; Ding et al., 2012). Most of the skarn deposits are related to the porphyries, concentrated at the Early Cretaceous, similar to the timing of porphyry deposits (Figure 8).

The three reported orogenic Au deposits also formed during the Cretaceous (Figure 8). Their ages are dated from the hydrothermal minerals. The hydrothermal zircons at Shangxu yielded a U–Pb age of ca. 119 Ma (Huang et al., 2012; Huang et al., 2021); biotite from Zhagela gave a K–Ar age of ca. 111–95 Ma (Liu et al., 2014); K-feldspar and sericite at Dacha display consistent K–Ar ages of 96 Ma, whereas the plagioclase K–Ar age is 94 Ma, which are all younger than the porphyry age of ca. 104 Ma (Ma et al., 2017), suggesting no connection between the porphyry intrusions and orogenic Au mineralization.

The timing of ophiolite-related Cr and Ni deposits has not been well constrained. Three of the five deposits have reported ages. One chromite Re–Os age was dated at 244 Ma in the Dongqiao deposit, which is older than the age of gabbro at 187 Ma (She et al., 2009; Shi et al., 2012; Wang et al., 2016a; Wei et al., 2016; Shi, 2017). Ophiolite in the Bangonghu deposit yielded U–Pb ages of 190–160 Ma (Wang et al., 2016a), whereas diabase in the Yilashan gave U–Pb ages of 183–170 and 133–114 Ma (Zhong et al., 2018). These mafic rocks are all younger than the chromite age, suggesting they may not have the same origin. The two quartz-vein W deposits in Jiagang and Jiaoxi were dated at 21 Ma and 11 Ma. Therefore, the molybdenite Re–Os ages are consistent with the U–Pb ages of the monazite granite of these two deposits (Figure 8; Wang et al., 2006a; Wang et al., 2006b; Wang et al., 2018b).

4.2 Relationship with tectonic evolution

As presented previously, the BNMB includes a subduction–accretionary complex, migrated magmatic arcs, major listric faults, large or basement-cored anticlines, deformed rigid basement blocks, and volcano-tectonic basins on both the northern margin of the Lhasa Terrane and the southern margin of the Qiangtang Terrane in the northern Tibetan Plateau (Song et al., 2014; Lin et al., 2021). Therefore, the definition of the BNMB involves the deposits on both sides of the BNSZ that have been recognized as products of subduction or post-subduction lithospheric extension, including the southern edge of the SQB, the BNSZ, and parts of the NLB and CLB.

Lin et al. (2021) comprehensively summarized the metallogeny of the BNMB and divided the BNMB into the western (west of 86° E), central (86° E to 94° E), and eastern (east of 94° E) regions, which represent different mineralization systems. They suggested that the mineralization of the BNMB may extend to the Yunnan province. However, the evolution of the BNO plays an important role for understanding the linkage between the formation of the Tibetan Plateau and the BNMB metallogeny. Yin and Harrison (2000) believed that ophiolite associated with the BNSZ was formed in a narrow basin that existed between the Lhasa and Qiangtang blocks during the Early Mesozoic (perhaps created by the subduction of Songpan–Ganzi to the north) and that minimal subduction was associated with the closure of this basin. Pan et al. (2012) proposed a model of a southern Qiangtang Paleozoic accretionary arc-basin system, revealing the BNO to be a large ocean containing numerous islands from the India Plate to the Eurasian Plate. Zhu et al. (2016) proposed a divergent double subduction model, emphasizing two Jurassic–Cretaceous magmatic arcs and an arc-arc "soft" collision between the Qiangtang and Lhasa Terranes. The opening and closure processes of the BNO have been clearly reconstructed from previous work, which provides a significant insight for the geodynamic background of the BNMB (Li et al., 2017b; Li et al., 2019d). Here, we will discuss the relationship between metallogeny and tectonic evolution, summarized in Figure 9.

Stage 1 (ca. 240–165 Ma): Continental rifting of Gondwana started in the Early Carboniferous and peaked in the Permian, leading to the breakup of the supercontinent and opening of several oceanic basins (Zeng et al., 2019). In the Middle-Late Triassic, a new tectonic style affected the Qiangtang and Lhasa Terranes: the BNO initially opened, recording the earliest instance of oceanic crust (Song et al., 2019a). A few Cr deposits were formed at this stage. Some evidence also showed that the Dongqiao and Yilashan chromite deposits experienced the early mid-ocean ridge expanding (MORB basalts) environment to the late subduction zone (SSZ-type ophiolite) multistage formation process (Dong et al., 2013; Duan et al., 2013; Zhang et al., 2018a; Zhang et al., 2018b; Zhang et al., 2019a; Zhang et al., 2019b; Dong et al., 2019; Bi et al., 2020). Therefore, the initial enrichment of chromium was promoted during the expansion of the BNO.

Stage 2 (ca. 165–145 Ma): Divergent double subduction of the BNO lithosphere initiated in the Middle- Late Jurassic (165–145 Ma) (Li et al., 2019b; Li et al., 2019c) and experienced episodic low-angle subduction and slab rollback that produced widespread granitoid from the Middle Jurassic (ca. 165 Ma) (Liu et al., 2020) to the Late Jurassic (ca. 145 Ma) (Hu, 2013; Li et al., 2013). A large amount of water may have existed in the subduction zone, which increased the activity of Cr (Dick and Bullen, 1984; Ballhaus, 1998) to locally form the podiform chromite ore, where primitive olivine–chromite-saturated mantle melt was sufficiently water-rich to exsolve fluids through the uppermost mantle (Matveev and Ballhaus, 2002). The most likely geodynamic environment for podiform chromite mineralization was a subduction-related setting within the BNO. Shi et al. (2012) suggested that the ophiolitic harzburgites and podiform chromites of the Dongqiao SSZ (suprasubduction zone type) ophiolite were formed from metasomatic refertilization of depleted Mesoproterozoic to Archean lithospheric mantle by Jurassic subduction melts. However, Kapp and DeCelles (2019) suggested that the earliest subduction-related magmatism emplaced on the northern Lhasa subterrane at ca. 170 Ma, indicating the initiation timing of the southward subduction of the BNO. The continued northward subduction of the BNO from 165 Ma led to the underplating of the mantle-derived basaltic magmas beneath SQB that provided heat and materials for the remobilization and anatexis of ancient crust, resulting in the formation of skarn Fe deposits. However, due to the limited supply of mantle components, the relatively reduced states,

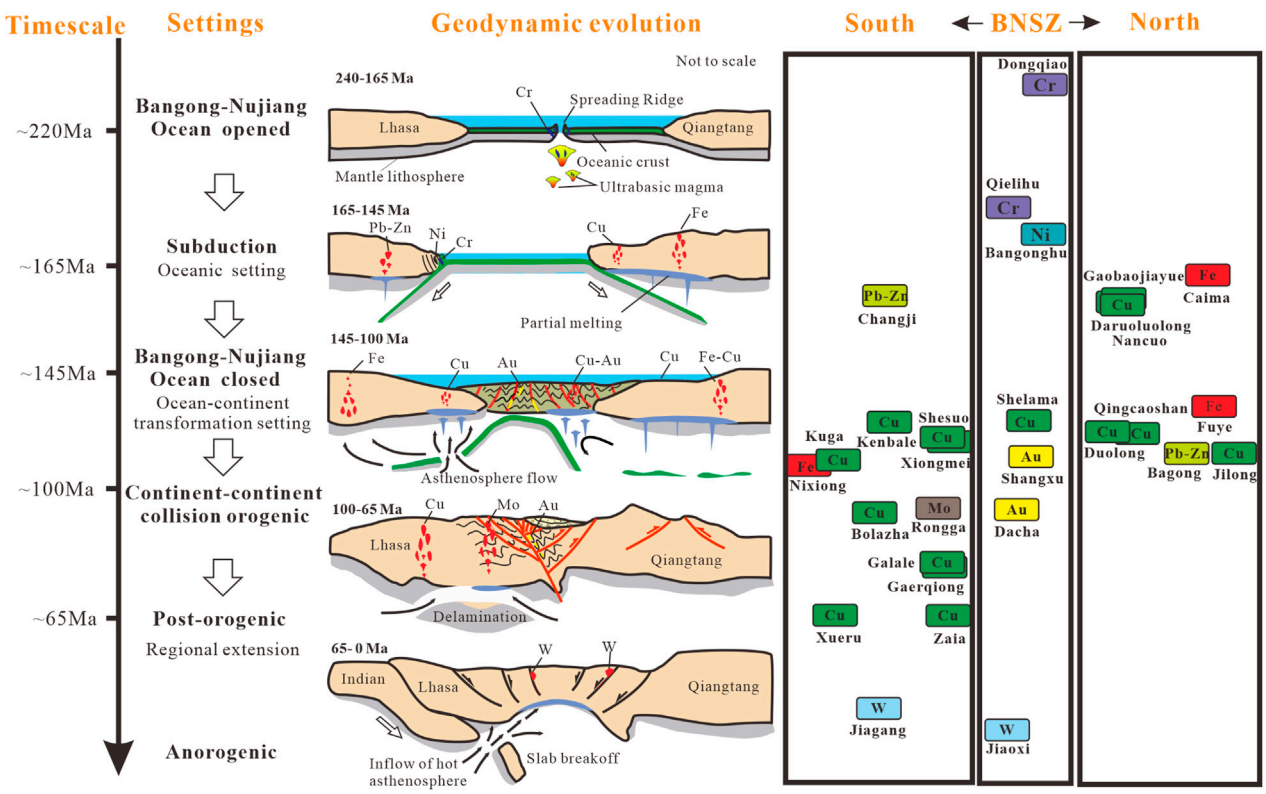

FIGURE 9
Geodynamic evolution and mineralization of the Bangong–Nujiang metallogenic belt.

and the highly evolved characteristics, the magmatic event in this period are unfavorable for the formation of large porphyry copper–gold deposits (Li et al., 2018). The Daruoluolong copper deposit is the oldest late Jurassic copper mineralization (ca. 155 Ma) discovered in the middle section of the BNMB. Three late Jurassic porphyries in Daruoluolong are derived from the lower crust by differentiation of depleted mantle during the northward subduction of the BNO (Gao et al., 2011; Gao et al., 2016; Geng et al., 2016; Gao et al., 2018; Gao et al., 2020). Song et al. (2019a) believed that the BNO was stable during the Middle Jurassic, whereas it reduced to a residual sea during the Late Jurassic to Early Cretaceous, according to the regional geological evidence.

Stage 3 (ca. 145–100 Ma): The BNO turned to coexisting arc–arc "soft" collision and subduction settings (Zhu et al., 2016; Song et al., 2019a) that varied at different locations between the Qiangtang and Lhasa Terranes. The final closure of the BNO and subsequent Lhasa–Qiangtang "soft" collision may have occurred during the latest Jurassic to Early Cretaceous (ca. 140–130 Ma) (Zhu et al., 2016). Note that the BNO is a branch of the Mesozoic Neo-Tethys Ocean. Thus, the closure of the BNO is characterized by the disappearance of oceanic crust. However, the subduction was still in progress at this time; the uplift of the continent crust and the slab roll-back formed the residual oceanic basin and subduction-related ore deposits (e.g., Duolong ore cluster; Sun et al., 2015; Song et al., 2015; Sun et al., 2017; Song et al., 2019a; Lin et al., 2018b). The Neo-Tethys Mesozoic subduction from 145 to 100 Ma is the ideal setting for the porphyry–skarn–epithermal deposits in the BNMB, similar to the tectonic background of the Andean metallogenic belt in South America (Mpodozis and Cornejo, 2012). Therefore, we believe that the fertility of the porphyry copper system could have occurred on both sides of the BNSZ. The accretionary wedge, along with the northward subduction of the Bangong–Nujiang oceanic crust, provides the main geological background for the formation of the Duolong world-class ore cluster. All deposits in the Duolong district are associated with the Early Cretaceous (123–115 Ma) intermediate-felsic porphyries (Lin et al., 2019a; Lin et al., 2019b; Yang et al., 2020a) and are characterized by abundant F, Cl, Cu, and Au in a high oxidation state. These intermediate-felsic porphyries contributed to the formation of the Duolong porphyry Cu–Au deposit (Li et al., 2013; Li et al., 2014; Li et al., 2015; Li et al., 2016). Regional deformation and faults during this period are also helpful for Cu and Au transportation and precipitation (Lin et al., 2020b).

Stage 4 (ca. 100–65 Ma): The collision between the Lhasa and Qiangtang terranes resulted in a significant crust thickening of the Middle and Late Cretaceous, which is evidenced by the lack of oceanic rocks, development of thrust faults, and collision-related magmatism (Song et al., 2019a; Lin et al., 2022). The Ga'erqiong, Galale, and Balazha skarn Cu deposits in NLB and CLB may have been formed in a transitional tectonic setting varying from collisional orogeny to extension in the early Late Cretaceous (Wang et al., 2013; Wang et al., 2019a). The collision-related porphyry Cu deposits developed in the BNMB are characterized by high-Mg# adakitic magmatic rocks. Those adakitic rocks

originated from partial melting of the delaminated juvenile crust that was modified by the subducted ocean slab-derived fluids (Wang et al., 2019a). Partial melting of the juvenile mafic crust, modified by the previously northward subducted BNO slab, provided the necessary ore metals and the ideal initial adakitic magmas for the Late Cretaceous porphyry–skarn deposit (Wang et al., 2019a). The metamorphic fluids related to regional deformation and thrust faults during the orogeny can remobilize the Au and form orogenic Au deposits (Feng et al., 2007; Fei et al., 2015).

Stage 5 (ca. 65–0 Ma): After the closure of the BNO (ca. 100 Ma) and the Yarlung Tsangpo Ocean (ca. 65 Ma), the dynamic setting turned to extension, which resulted in the formation of the tungsten deposits (18–15 Ma). Anatexis of the ancient crust and subsequent fractional crystallization could result in the substantial accumulation of tungsten in the melts and the high degree of fractional crystallization of the crustal-derived magmas with a relatively low magmatic oxidation state. This process is recognized as a critical step in the development of tungsten mineralization (Wang et al., 2018a; Xu et al., 2020).

5 Implications for exploration

5.1 Porphyry–skarn–epithermal copper polymetallic deposits

The BNO opened in the Middle and Late Triassic, which is consistent with the closure of the Paleo-Tethys Ocean (Song et al., 2019b; Zeng et al., 2020). Increasing amounts of evidence support that the regional uplift and sea water retreated in the BNO between 110 and 100 Ma (e.g., Tang and Tao, 2009; Li et al., 2020a). The magmatism of 160–150 Ma associated with skarn Cu–Fe mineralization on both sides of the BNSZ is important, similar to the Daruoluolong, Nancuo, and Gaobaojiayue deposits. Therefore, another Early Cretaceous "Duolong" porphyry–epithermal deposit in the northern part of the BNMB potentially existed, and more porphyry–skarn copper polymetallic deposits along the continental margin arcs are of great potential for prospecting.

The post-ore weathering and denudation probably influence the final grade and economic value of epithermal deposits (Hedenquist et al., 2000). Due to the inevitable erosion of the Tibetan Plateau, the formation and discovery of Mesozoic porphyry–epithermal deposits require a more comprehensive understanding of the exhumation history. The newly explored Tiegelongnan Cu(–Au) deposit is a massive, superimposed porphyry–epithermal deposit that was covered by post-ore Meiriqiecuo Group volcanic rocks (Tang et al., 2017; Song et al., 2018; Yang et al., 2020a; Yang et al., 2020b; Yang et al., 2020c). After brief erosion, epithermal Cu–Au and porphyry Cu ore bodies were preserved at Tiegelongnan, with a minimum erosional thickness of 500–600 m and the potential for new discoveries at depth (Song et al., 2018). The Early Cretaceous volcanic cover and Late Cretaceous thrust faults have a dual effect on the preservation of the ore body in the Duolong district (Song et al., 2019b). In summary, the BNO is an ancient ocean that has undergone a long evolutionary history of ca. 120 Ma (235–110 Ma). The magmatism in both sides of the BNMB and the large volume of volcanic rocks (Meiriqiecuo, Zenong, and Duoni formations) during the subduction of the BNO suggest that more porphyry–skarn–epithermal deposits might be found in the BNMB.

5.2 Orogenic gold deposits

Central Tibet experienced a gold mining rush during the 1990s. Bafflingly, no economically valuable hypogene gold deposit has been found (Song et al., 2014; Geng et al., 2015). Integrated with earlier studies, we think the accretive wedges and post-collision strike-slip faults in the BNSZ may be favorable sites for orogenic gold mineralization (Song et al., 2014), which is supported by the study of the Shangxu deposit, hosted by the oceanic flysch of the Mugagangri Group (Fang et al., 2020a; Fang et al., 2020b; Fang et al., 2020c). The Mugagangri Group intermittently outcropped in a length of more than 1,000 km in the BNSZ. The ductile shear zones that widely developed in the Mugagangri Group contain a few gold deposits (prospection), such as Shangxu, Dacha, and Daze. Orogenic gold deposits in the BNMB are not entirely controlled by accretionary wedge melange or post-collision strike-slip faults. Although the Mugagangri Group in the Shangxu gold deposit experienced intense deformation, the metamorphic degree is at low greenschist facies, which belongs to the shallow crustal environment. The magma that existed at depth provided ore-forming materials, heat sources, and fluids and also extracted ore-forming materials from surrounding rocks during ascent of hydrothermal fluids, resulted in large orogenic gold deposits (Fang et al., 2020c). Therefore, we believe that the post-collision strike-slip fault and the recombination of the rock mass in the Mugagangri Group at the initial stage of the collision may be favorable locations for orogenic gold deposits in the BNSZ.

5.3 Quartz-vein tungsten deposits

The wolframite resources in the BNMB have recently drawn extensive attention due to their economic significance and very young ages. Wang et al. (2016b), Wang et al. (2018a) argued that the Jiaoxi W deposit in the BNMB originated from magmatic-hydrothermal fluids. The geological work shows that the Jiaoxi deposit mainly developed the veinlet zone and the veinlet-large vein mixed zone according to the "Five levels" model. However, the line vein zone at the top and the large vein zone in the deep part were not observed (Xu et al., 2008; Wang et al., 2010). The absence of the top vein zone may be related to the strong uplift and denudation in Tibet. Due to the strong denudation, more 0.5-m-wide veins (No. 18 and No. 8 ore bodies) have been exposed to the surface, while the absence of the deep vein zone may be related to the relative lack of detailed research at present, given that only two drillings have been completed, and the deep ore bodies have not been completely identified by the boreholes. Therefore, it is of great economic significance to find the large vein zone in the deep part of the deposit.

5.4 Porphyry molybdenum deposits

The discovery of the Rongga molybdenum deposit adds new mineralization types to the southern margin of the BNMB,

indicating that there are porphyry molybdenum deposits related to the collision setting. The Mo-rich oceanic sediment melts and subsequent crystallization differentiation are the main reasons for the Mo enrichment of ore-bearing porphyry (Peng et al., 2019). For this reason, it may be a favorable target for the exploration of molybdenum deposits in the Jurassic–Cretaceous marine stratum distribution area of the southern margin of the BNMB.

6 Implications for future work

There are several implications for future work based on the aforementioned summary and reviews:

(1) The accurate geochronology of significant tectonic events, including the opening of the BNO, the initial oceanic subduction, the Lhasa–Qiangtang collision, and the orogenic uplift, should be more precisely constrained. Particularly, clarification of the subduction polarity, tectonic evolution to oceanic subduction and continental collision, and establishment of the chronological framework are essential.
(2) A genetic linkage between magmatism and mineralization is crucial to determining the deployment of national geological work. Accordingly, magma episodes, tectonic evolution, deep dynamic processes, and metal and magma sources should be analyzed.
(3) The history of the discovery and research of many deposits in the BNMB is short, mostly less than 10 years. Thus, the exploration and understanding of detailed geology and genesis of mineral deposits in the BNMB are in an early stage. It is essential to study the typical deposits in the BNMB, particularly the porphyry copper system and orogenic gold deposits. In terms of the regional metallogeny, detailed research should be performed on metal sources, the evolution of hydrothermal fluids, metal transportation and precipitation, and deposit preservation, with the ultimate goal of establishing a regional exploration model.

7 Conclusion

Metal reserves and average grades of 57 deposits (or prospects) were first reported and reviewed here. The temporal–spatial distribution of the BNMB is redefined from the Permian to Miocene in this paper. Porphyry copper deposits, skarn copper–iron deposits, orogenic gold deposits, ophiolite-related chromite and nickel deposits, and quartz-vein-type and greisen-type tungsten deposits are well developed in the BNMB. These major deposits had been recognized as the products of subduction or collision on both sides of the BNSZ. Porphyry–epithermal copper, orogenic gold, and skarn copper deposits in the subduction setting are the deposit types with the most potential for future exploration. In addition, more attention should be paid to the discovery of post-collision (<100 Ma) Mo–W mineralization.

Author contributions

YS developed the overall structure of the manuscript, collected most of the data, and wrote most sections of the manuscript. JT contributed to the Introduction section and provided invaluable comments for the conception of the manuscript. BL wrote most of the Regional Geology section and provided useful insights for the manuscript. CY contributed to the Metallogeny section and processed some data and figures. HS contributed to the figure processing and references of the manuscript.

Funding

This study was funded by the National Natural Science Foundation of China (Grant No. 42172100), the China Geological Survey project (Grant No. DD20190617), the National Key R&D Program of China (Grant No. 2022YFC2905001), and the Innovative Youth Talents Program, Ministry of Natural Resources (YS, Grant No. KY-BR-XZ-202006).

Acknowledgments

From 2003 to 2022, the China Geological Survey (CGS) and the Tibet Geological Exploration Bureau (TGEB) carried out collaborative geological survey and mineral resource prospecting. YS thanks Georges Beaudoin for inviting him to visit Laval University and inspect the world famous Abitibi greenstone belt that inspired this review. An early draft of this manuscript also benefitted greatly from discussion and comments from Georges Beaudoin. We also thank Huan Li and Liang Qiu for their insightful comments, which greatly improved the manuscript.

Conflict of interest

The authors declare that the research was conducted in the absence of any commercial or financial relationships that could be construed as a potential conflict of interest.

Publisher's note

Supplementary material

The Supplementary Material for this article can be found online at: https://www.frontiersin.org/articles/10.3389/feart.2023.1139941/full#supplementary-material

References

Ballhaus, C. (1998). Origin of podiform chromite deposits by magma mingling. *Earth Planet. Sci. Lett.* 156 (3), 185–193. doi:10.1016/S0012-821X(98)00005-3

Bi, Z., Wang, Y., Sun, X., Zhang, J., Zhang, T., and Liu, T. (2020). Geological characteristics, magmatic geochemistry and petrogenic chronology of the Bagong Pb polymetallic ore spot in Ritu County, Tibet. *Geol. China.* 47 (2), 497–515.

Dick, H. J. B., and Bullen, T. (1984). Chromian spinel as a petrogenetic indicator in abyssal and alpine-type peridotites and spatially associated lavas. *Contrib. Mineral. Petrol.* 86 (1), 54–76. doi:10.1007/BF00373711

Ding, L., Zhao, Y., Yang, Y., Cui, Y., and Lv, L. (2012). LA-ICP-MS zircon U-Pb dating and geochemical characteristics of ore-bearing granite in skarn-type iron polymetallic deposits of Duoba area, Baingoin County, Tibet, and their significance. Acta Petrol. *Mineral.* 31 (4), 479–496.

Ding, S., Chen, Y., Tang, J., Zheng, W., Lin, B., and Yang, C. (2017). Petrogenesis and tectonics of the Naruo porphyry Cu (Au) deposit related intrusion in the Duolong area, central Tibet. *Acta Geol. sin-engl.* 91 (2), 581–601. doi:10.1111/1755-6724.13119

Dong, L., Li, G., Huang, H., and Yong, Y. (2013). Geochemical characteristics, chronology and the significance of Laqing copper polymetallic skarn deposit, Bange county, Tibet. *Geol. Bull. China.* 32 (5), 767–773.

Dong, Y., Yang, J., Lian, D., Xiong, F., Zhao, H., Chen, X., et al. (2019). Genesis and tectonic setting of the Dongqiao peridotites in the central segment of the Bangong Co-Nujiang Suture Zone. *Geol. China* 46 (1), 87–114. doi:10.12029/gc20190106

Duan, Z., Li, G., Zhang, H., Li, Y., and Duan, Y. (2013). Zircon U-Pb age and geochemical characteristics of the quartz monzobiorite and metallogenic background of the Sena gold deposit in Duolong metallogenic concentrated area, Tibet. *J. Jilin Univ. Earth Sci. Ed.* 43 (6), 1864–1877. doi:10.13278/j.cnki.jjuese.2013.06.014

Fang, X., Song, Y., Tang, J., Wang, J., and Li, H. (2020b). Metallogenic epoch study on the Shangxu gold deposit, Bangong-Nujiang suture zone, Tibet and its geological implications. *Acta Geol. Sin. Chin. Ed.).* 94, 3376–3390. doi:10.19762/j.cnki.dizhixuebao.2020168

Fang, X., Tang, J., Beaudoin, G., Song, Y., and Chen, Y. (2020a). Geology, mineralogy and geochemistry of the Shangxu orogenic gold deposit, central Tibet, China: Implications for mineral exploration. *Ore Geol. Rev.* 120, 103440. doi:10.1016/j.oregeorev.2020.103440

Fang, X., Tang, J., Song, Y., Beaudoin, G., Yang, C., and Huang, X. (2020c). Genesis of the Shangxu orogenic gold deposit, Bangong-Nujiang suture belt, central Tibet, China: Constraints from H, O, C, Si, He and Ar isotopes. *Ore Geol. Rev.* 127, 103810. doi:10.1016/j.oregeorev.2020.103810

Fei, F., Yang, Z., Liu, Y., Zhao, X., and Yu, Y. (2015). Petrogenetic epoch of the rock mass in the Lunggar iron deposit of Coqen County, Tibet. *Acta Petrol. Mineral.* 34, 568–580. doi:10.3969/j.issn.1000-6524.2015.04.010

Feng, G., Chen, Z., Liao, L., and Xiao, Y. (2007). Geological characteristics of the Fuye porphyrite iron deposit, Rutog County, Tibet, China and its significance for iron prospecting. *Geol. Bull. China.* 26 (8), 1042–1047. doi:10.3969/j.issn.1671-2552.2007.08.018

Gao, K., Song, Y., Liu, Z. B., Fang, X., Li, F., and Li, H. (2018). Petrogenesis and tectonic significance of the three-period porphyries from the Daruoluolong Cu (Au) deposit, Tibet, China. *Acta Geol. Sin. Engl. Transl.).* 92 (3), 1267–1269. doi:10.1111/1755-6724.13610

Gao, K., Tang, J., Song, Y., Liu, Z., Fang, X., Yang, H., et al. (2016). Fluid inclusion study of the cryptoexplosive breccias in the Naruo Cu (Au) deposit of Tibet. *Geol. Prospect.* 52 (5), 0815–0825. doi:10.13712/j.cnki.dzykt.2016.05.002

Gao, S., Zheng, Y., Jiang, X., Li, W., and Jiang, J. (2020). Discovery, Genesis and significances of first siver-tin polymetal deposit in Western Gangdese belt. *Earth Sci.* 45 (12), 4463–4480.

Gao, S., Zheng, Y., Xie, M., Zhang, Z., Yan, X., Wu, B., et al. (2011). Geodynamic setting and mineralizational implication of the Xueru intrusion in ban'ge, Tibet. *Earth Sci. Wuhan. China)* 36 (4), 729–739. doi:10.3799/dqkx.2011.073

Ge, L., Zou, Y., and Xing, J. (2004). Discovery of the Jiagang Snow Mountain tungsten-molybdenum-copper-gold polymetallic occurrence in the northern part of the Gangdise block, Tibet. *Geol. Bull. China.* 23 (9~10), 1033–1039. doi:10.3969/j.issn.1671-2552.2004.09.029

Geng, Q., Mao, X., Zhang, Z., Peng, Z., and Guan, J. (2015). New understanding in the middle and west part of Bangong lake-nujiang river metallogenic belt and its lmplication for prospecting. *Geol. Surv. China.* 2 (2), 1–11. doi:10.19388/j.zgdzdc.2015.02.002

Geng, Q., Zhang, Z., Peng, Z., Guan, J., Zhu, X., and Mao, X. (2016). Jurassic-Cretaceous granitoids and related tectono-metallogenesis in the Zapug–Duobuza arc, Western Tibet. *Ore Geol. Rev.* 77, 163–175. doi:10.1016/j.oregeorev.2016.02.018

Hedenquist, W., Arribas, A. R., and Gonzalez-Urien, E. (2000). Exploration for epithermal gold deposits. *Econ. Geol.* 13, 245–277. doi:10.5382/Rev.13.07

Hou, Z., Ma, H., Khin, Z., Zhang, Y., Wang, M., Wang, Z., et al. (2003). The himalayan yulong porphyry copper belt: Product of large-scale strike-slip faulting in eastern Tibet. *Econ. Geol.* 98 (1), 125–145. doi:10.2113/gsecongeo.98.1.125

Hou, Z., Zaw, K., Pan, G., Mo, X., Xu, Q., Hu, Y., et al. (2007). Sanjiang Tethyan metallogenesis in S.W. China: Tectonic setting, metallogenic epochs and deposit types. *Ore Geol. Rev.* 31 (1), 48–87. doi:10.1016/j.oregeorev.2004.12.007

Hou, Z., and Zhang, H. (2015). Geodynamics and metallogeny of the eastern Tethyan metallogenic domain. *Ore Geol. Rev.* 70, 346–384. doi:10.1016/j.oregeorev.2014.10.026

Hou, Z., Zheng, Y., Lu, Z., Xu, B., Wang, C., and Zhang, H. (2020). Growth, thickening and evolution of the thickened crust of the Tibet Plateau. *Acta Geol. Sin.* 94 (10), 2797–2815. doi:10.19762/j.cnki.dizhixuebao.2020199

Hu, W. (2013). Geological characteristics and their prospecting significance of Fuye iron deposit in Ritu county, Tibet. *East China Geol.* 34 (1), 29–37. doi:10.3969/j.issn.1671-4814.2013.01.005

Huang, H., Li, G., Liu, B., Dong, S., Shi, H., Zhang, Z., et al. (2012). Zircon U-Pb geochronology and geochemistry of the tiangongnile skarn-type Cu-Au deposit in zhongba county, Tibet: Their genetic and tectonic setting significance. *Acta Geosci. Sin.* 33 (4), 424–434.

Huang, H., Li, G., Liu, B., Zhang, Z., Ma, D., Qu, Z., et al. (2014). Discovery of Shangxu orogenic type gold deposit in northern Tibet and its significance. *Min. Deposits.* 33 (3), 486–496. doi:10.16111/j.0258-7106.2014.03.013

Huang, H., Luosang, J., Dai, Z., Liu, H., Fu, J., Li, G., et al. (2021). Hydrothermal zircon geochronology in the Shangxu gold deposit and its implication for the Early Cretaceous orogenic gold mineralization in the middle Bangonghu–Nujiang suture zone. *Acta Geol. Sin. Engl. Transl.).* 95 (04), 1249–1259. doi:10.1111/1755-6724.14679

Kapp, P., DeCelles, P. G., Gehrels, G. E., Heizler, M., and Ding, L. (2007). Geological records of the lhasa–qiangtang and indo-asian collisions in the nima area of central Tibet. *Geol. Soc. Am. Bull.* 119, 917–933. doi:10.1130/B26033.1

Kapp, P., and DeCelles, P. G. (2019). Mesozoic–Cenozoic geological evolution of the Himalayan-Tibetan orogen and working tectonic hypotheses. *Am. J. Sci.* 319 (3), 159–254. doi:10.2475/03.2019.01

Kapp, P., Murphy, M. A., Yin, A., Harrison, T. M., Ding, L., and Guo, J. R. (2003). Mesozoic and cenozoic tectonic evolution of the shiquanhe area of Western Tibet. *Tectonics* 22, 1029. doi:10.1029/2001TC001332

Lai, W., Hu, X., Garzanti, E., Sun, G., Garzione, C., Marcelle, B., et al. (2019). Initial growth of the northern lhasaplano, Tibetan plateau in the early late cretaceous (ca. 92 Ma). *Geol. Soc. Am. Bull.* 131 (11-12), 1823–1836. doi:10.1130/B35124.1

Lei, M., Chen, J., Xu, J., Zeng, Y., and Xiong, Q. (2019). Late Cretaceous magmatism in the NW Lhasa Terrane, southern Tibet: Implications for crustal thickening and initial surface uplift. *Geol. Soc. Am. Bull.* 132 (1-2), 334–352. doi:10.1130/B31915.1

Li, B., Fan, H., Zhu, D., Peng, B., Guo, P., and Zhou, L. (2020a). Geochemical characteristics, detrital zircon U-Pb geochronology, and its tectonic significance for the Jingzhushan Formation from northern region of Geji County, northern Tibet. *Acta Geol. Sin.* 94 (12), 3657–3673. doi:10.19762/j.cnki.dizhixuebao.2020051

Li, B., Qu, X., Ma, X., Chen, W., and Sun, M. (2020b). Chronology,types and Genesis of post-collisional copper bearing magmatic rocks in the Xiongmei area,the middle part of the Bangong Co-Nujiang metallogenic belt. *Acta Geol. Sin. Chin. Ed.).* 94 (4), 1264–1281. doi:10.19762/j.cnki.dizhixuebao.2019178

Li, C., Zhai, Q., Dong, Y., Liu, S., Xie, C., and Wu, Y. (2009). High-pressure eclogite-blueschist metamorphic belt and closure of paleo-Tethys Ocean in Central Qiangtang, Qinghai-Tibet plateau. *Earth Sci.* 20, 209–218. doi:10.1007/s12583-009-0021-4

Li, D. (2012). "Study on the fluid inclusions of the bolong copper deposit, Tibet," master's thesis. (Chengdu: Chengdu University of Technology).

Li, G., Ding, L., Guilmette, C., Fu, J., Xu, Q., Yue, Y., et al. (2017b). The subduction-accretion history of the Bangong-Nujiang Ocean: Constraints from provenance and geochronology of the Mesozoic strata near Gaize, central Tibet. *Tectonophysics* 702, 42–60. doi:10.1016/j.tecto.2017.02.023

Li, G., Li, J., Qin, K., Duo, J., Zhang, T., Xiao, B., et al. (2012). Geology and hydrothermal alteration of the Duobuza gold-rich porphyry copper district in the bangongco metallogenetic belt, northwestern Tibet. *Resour. Geol.* 62 (1), 99–118. doi:10.1111/j.1751-3928.2011.00182.x

Li, G., Qin, K., Li, G., Noreen, J., E., Zhao, J., Cao, M., et al. (2016). The Nadun Cu-Au mineralization, central Tibet: Root of a high sulfidation epithermal deposit. *Ore Geol. Rev.* 78, 371–387. doi:10.1016/j.oregeorev.2016.04.019

Li, G., Qin, K., Li, J., Noreen, J., E., Zhao, J., Cao, M., et al. (2017a). Cretaceous magmatism and metallogeny in the Bangong-Nujiang metallogenic belt, central Tibet: Evidence from petrogeochemistry, zircon U-Pb ages, and Hf-O isotopic compositions. *Gondwana Res.* 41, 110–127. doi:10.1016/j.gr.2015.09.006

Li, G., Qin, K., Li, J., Noreen, J., Zhao, J., Cao, M., et al. (2011). High-temperature magmatic fluid exsolved from magma at the Duobuza porphyry copper-gold deposit, Northern Tibet. *Geofluids* 11 (2), 134–143. doi:10.1111/j.1468-8123.2011.00325.x

Li, H., Li, C., Gao, Y., and Zeng, M. (2019b). Geochronology and geochemistry characteristics of the late Mid-Jurassic (ca. 163Ma) OIB-type diabase and high-Mg diorites in Shiquanhe ophiolite: Products of early stage oceanic crust subduction? *Acta Petrol Sin.* 35 (03), 816–832. doi:10.18654/1000-0569/2019.03.12

Li, H., Liu, Z., Chen, W., Wang, N., Wang, J., Zhang, K., et al. (2019c). The discovery of high-Mg rhyolitic rocks in Peng Tso area, Tibet and its significance for evolution of Bangong-Nujiang Ocean. *Acta Petrol Sin.* 35 (3), 799–815. doi:10.18654/1000-0569/2019.03.11

Li, H., Zhong, W., Guo, J., Qin, Z., Zhang, Z., Li, J., et al. (2019d). Petrogenesis of igneous rocks and ore-forming material source of the Nating porphyry Cu (Au) deposit in the Western section of the Bangong Co-Nujiang metallogenic belt, Tibet. *Acta Petrol. Sin.* 35 (6), 1717–1737. doi:10.18654/1000-0569/2019.06.06

Li, J., Li, G., Qin, K., and Xiao, B. (2008). Geochemistry of porphyries and volcanic rocks and ore-forming geochronology of Duobuza gold-rich porphyry copper deposit in Bangonghu belt, Tibet: Constraints on metallogenic tectonic settings. *Acta Petrol. Sin.* 24 (3), 531–543.

Li, J., Qin, K., Li, G., Jeremy, P. R., Zhao, J., and Cao, M. (2014). Geochronology, geochemistry, and zircon Hf isotopic compositions of mesozoic intermediate–felsic intrusions in central Tibet: Petrogenetic and tectonic implications. *Lithos* 198, 77–91. doi:10.1016/j.lithos.2014.03.025

Li, J., Qin, K., Li, G., Xiao, B., Zhao, J., Cao, M., et al. (2013). Petrogenesis of ore-bearing porphyries from the Duolong porphyry Cu–Au deposit, central Tibet: Evidence from U-Pb geochronology, petrochemistry and Sr-Nd-Hf-O isotope characteristics. *Lithos* 160-161, 216–227. doi:10.1016/j.lithos.2012.12.015

Li, S., Xiao, R., Zhou, S., Mo, X., Shen, J., Yan, B., et al. (2005). Gold mineralization in gaize area, Tibet. *Min. Deposits*. 24 (1), 1–14. doi:10.3969/j.issn.0258-7106.2005.01.001

Li, X., Chen, J., Wang, R., and Li, C. (2018). Temporal and spatial variations of Late Mesozoic granitoids in the SW Qiangtang, Tibet: Implications for crustal architecture, Meso-Tethyan evolution and regional mineralization. *Earth-Sci. Rev.* 185, 374–396. doi:10.1016/j.earscirev.2018.04.005

Li, X., Li, C., Sun, Z., and Wu, H. (2015). Zircon U-Pb geochronology, Hf isotope, and whole-rock geochemistry of diorite in the Saijiao Cu-Au deposit, Tibet, and its ore-forming significance. *Geol. Bull. China.* 34 (5), 908–918. doi:10.3969/j.issn.1671-2552.2015.05.011

Liang, H., Sun, W., Su, W., and Zartman, R. (2009). Porphyry copper-gold mineralization at yulong, China, promoted by decreasing redox potential during magnetite alteration. *Econ. Geol.* 104, 587–596. doi:10.2113/gsecongeo.104.4.587

Liang, X., Wang, G., Yang, B., Ran, H., Zheng, Y., Du, J., et al. (2017). Stepwise exhumation of the Triassic Lanling high-pressure metamorphic belt in Central Qiangtang, Tibet: Insights from a coupled study of metamorphism, deformation, and geochronology. *Tectonics* 36 (4), 652–670. doi:10.1002/2016TC004455

Lin, B., Chen, Y., Tang, J., Song, Y., Wang, Q., Feng, J., et al. (2016). Zircon U-Pb geochronology and Hf isotopic composition of the ore bearing porphyry in Dibao Cu (Au) deposit, Duolong ore concentration area, Tibet, and its geological significance. *Geol. Rev.* 62 (6), 1565–1578. doi:10.16509/j.georeview.2016.06.015

Lin, B., Chen, Y., Tang, J., Song, Y., Wang, Q., He, W., et al. (2018a). Geology, alteration and mineralization of Tiegelongnan giant Cu (Au, Ag) deposit, Tibet. *Min. Deposits.* 37 (05), 917–939. doi:10.16111/j.0258-7106.2018.05.002

Lin, B., Fang, X., Wang, Y., Yang, H., and He, W. (2019b). Petrologic Genesis of ore-bearing porphyries in Tiegelongnan giant Cu (Au, Ag) deposit, Tibet and its implications for the dynamic of Cretaceous mineralization. *Duolong. Acta Petrol.* Sin. 35 (3), 642–664.

Lin, B., Song, Y., Liu, Z., Liu, Z., and Gao, Y. (2018b). New zircon U-Pb age of the ore-bearing porphyry from the Kuga copper deposit in the eastern Bangongco-Nujiang matallogenic belt, Tibet. *Acta Geol. Sin. Engl. Ed.).* 92 (2), 859–861. doi:10.1111/1755-6724.13561

Lin, B., Tang, J., Chen, Y., Baker, M., Song, Y., Yang, H., et al. (2019a). Geology and geochronology of Naruo large porphyry-breccia Cu deposit in the Duolong district, Tibet. *Gondwana Res.* 66, 168–182. doi:10.1016/j.gr.2018.07.009

Lin, B., Tang, J., Chen, Y., Song, Y., Hall, G., Wang, Q., et al. (2017). Geochronology and genesis of the tiegelongnan porphyry Cu (Au) deposit in Tibet: Evidence from U-Pb, Re-Os dating and Hf, S, and H-O isotopes. *Resour. Geol.* 67 (1), 1–21. doi:10.1111/rge.12113

Lin, B., Zhang, X. G., Tang, P., Wang, L. Q., Santosh, M., Xi, Z., et al. (2021). Geology and geochronology of the jinmuguo Mo polymetallic deposit: Implications for the metallogeny of the bangongco- Nujiang belt of Tibet. *Ore Geol. Res.* 139, 104460. doi:10.1016/j.oregeorev.2021.104460

Lin, B., Zou, B., Tang, P., He, W., Liu, Z. Y., Qi, J., et al. (2022). Multiple isotopic dating constrains the time framework (age) of a porphyry system: A case study from the sangri Cu-Mo deposit, bangongco-nujiang metallogenic belt, Tibet, China. *Ore Geol. Res.* 144, 104870. doi:10.1016/j.oregeorev.2022.104870

Liu, D., Shi, R., Ding, L., and Zou, H. (2018). Late Cretaceous transition from subduction to collision along the Bangong-Nujiang Tethys: New volcanic constraints from central Tibet. *Lithos* 296-299, 452–470. doi:10.1016/j.lithos.2017.11.012

Liu, H., Huang, Q., Uysal, I., Cai, Z., Wan, Z., Xia, B., et al. (2020). Geodynamics of the divergent double subduction along the Bangong-Nujiang tethyan suture zone: Insights from late mesozoic intermediate-mafic rocks in central Tibet. *Gondwana Res.* 79, 233–247. doi:10.1016/j.gr.2019.09.018

Liu, W., Zhao, J., Ji, Q., Zhang, M., Zhao, K., and Liu, C. (2014). Geological characteristics and petrogenesis of the Zhagela gold deposit in Dingqing, Tibet. *Acta Geol. Sin.* 49 (4), 1169–1183. doi:10.3969/j.issn.0563-5020.2014.04.009

Lv, L., Cui, Y., Song, L., Diao, Y., Qu, X., and Wang, J. (2011). Geochemical characteristics and zircon LA-ICP-MS U Pb dating of Galale skarn gold (copper) deposit, Tibet and its significance. *Earth Sci. Front.* 18 (5), 224–242. doi:10.1007/s11442-011-0836-7

Ma, G., Liu, H., Huang, H., Chen, M., Lan, S., Lu, M., et al. (2017). Metallogenic conditions and prospecting potential of orogenic gold deposits in the central Western part of Bangong Lake-Nujiang metallogenic zone. *Sediment. Geol. Tethyan Geol.* 37 (3), 89–95. doi:10.3969/j.issn.1009-3850.2017.03.011

Matveev, S., and Ballhaus, C. (2002). Role of water in the origin of podiform chromitite deposits. *Earth Planet. Sci. Lett.* 203 (1), 235–243. doi:10.1016/S0012-821X(02)00860-9

Mo, X., Niu, Y., Dong, G., Zhao, Z., Hou, Z., Zhou, S., et al. (2008). Contribution of syncollisional felsic magmatism to continental crust growth: A case study of the paleogene linzizong volcanic succession in southern Tibet. *Chem. Geol.* 250 (1-4), 49–67. doi:10.1016/j.chemgeo.2008.02.003

Mo, X., Zhao, Z., Deng, J., Dong, G., Zhou, S., Guo, T., et al. (2003). Response of volcanism to the India-Asia collision. *Earth Sci. Front.* 3, 135–148.

Moritz, R., and Baker, T. (2019). Metallogeny of the tethyan orogenic belt: From mesozoic magmatic arcs to cenozoic back-arc and postcollisional settings in southeast europe, anatolia, and the lesser caucasus: An introduction. *Econ. Geol.* 114 (7), 1227–1235. doi:10.5382/econgeo.4683

Mpodozis, C., and Cornejo, P. (2012). *Cenozoic tectonics and porphyry copper systems of the Chilean Andes*. United States: Society of Economic Geologists Special Publication, 329–360.

Pan, G., Mo, X., Hou, Z., Zhu, D., Wang, L., Li, G., et al. (2006). Spatial-temporal framework of the Gangdese orogenic belt and its evolution. *Acta Petrol. Sin.* 22 (3), 521–533. doi:10.3321/j.issn:1000-0569.2006.03.001

Pan, G., Wang, L., Li, R., Yuan, S., Ji, W., Yin, F., et al. (2012). Tectonic evolution of the qinghai-tibet plateau. *J. Asian Earth Sci.* 53, 3–14. doi:10.1016/j.jseaes.2011.12.018

Peng, B., Li, B., Liu, H., Qin, G., Gong, F., and Zhou, L. (2019). Main collisional mineralization of Bangong-Nujiang metallogenic belt, Tibet: Geochronological, geochemical and isotopic evidence from Rongga molybdenum deposit. *Acta Petrol. Sin.* 35 (3), 705–723. doi:10.18654/1000-0569/2019.03.06

Qiao, D., Zhao, Y., Wang, A., Li, Y., Guo, S., Li, X., et al. (2017). Geochronology, fluid inclusions, geochemical characteristics of Dibao Cu (Au) deposit, Duolong ore concentration area, Xizang (Tibet), and its genetic type. *Acta Geol. Sin.* 91 (7), 1542–1564. doi:10.19762/j.cnki.dizhixuebao.2017.07.009

Qu, C. (2016). The geologic characteristics and prospecting marks of the cuprum-gold polymetallic deposit in Shelama, Gaize country, Tibet province. *Geol. Fujian* 35 (1), 55–63.

Qu, X., Wang, R., Dai, J., Li, Y., Qi, X., Xin, H., et al. (2012). Integrated thermophilic submerged aerobic membrane bioreactor and electrochemical oxidation for pulp and paper effluent treatment-towards system closure. *Min. Deposits.* 31 (1), 1–8. doi:10.1016/j.biortech.2012.04.045

Qu, X., and Xin, H. (2006). Ages and tectonic environment of the Bangong Co porphyry copper belt in Western Tibet, China. *Geol. Bull. China.* 25 (7), 792–799. doi:10.3969/j.issn.1671-2552.2006.07.004

Qu, X., Zhao, Y., Wang, R., Li, Y., Xin, H., Dai, J., et al. (2009). Discovery of magmatic nickel sulfide mineralizations in Bangong Lake-Nujiang metallogenic belt, Qinghai-Tibet plateau. *Min. Deposits.* 28 (6), 729–736.

Richards, J. P. (2015). Tectonic, magmatic, and metallogenic evolution of the Tethyan orogen: From subduction to collision. *Ore Geol. Rev.* 70, 323–345. doi:10.1016/j.oregeorev.2014.11.009

She, H., Li, J., Ma, D., Li, G., Zhang, D., Feng, C., et al. (2009). Molybdenite Re-Os and SHRIMP zircon U-Pb dating of Duobuza porphyry copper deposit in Tibet and its geological implications. *Min. Deposits.* 28 (6), 737–746. doi:10.3969/j.issn.0258-7106.2009.06.003

Shi, C. (2017). "Study on the geological characteristics and enrichment regularities of mineralization of Nancuo gold polymetallic deposit in Amdo area, Tibet," master's thesis. (Jilin: Jilin University).

Shi, R., Griffin, W. L., O'Reilly, S. Y., Huang, Q., Zhang, X., Liu, D., et al. (2012). Melt/mantle mixing produces podiform chromite deposits in ophiolites: Implications of Re–Os systematics in the Dongqiao Neo-tethyan ophiolite, northern Tibet. *Gondwana Res.* 21 (1), 194–206. doi:10.1016/j.gr.2011.05.011

Song, J., Tang, J., Zhang, Z., Peng, Z., Lin, X., and Wang, Y. (2015). Characteristics of fluid inclusions and metallogenic process of Gaerqiong-Galale Cu-Au ore concentration area. *Tibet. Min. Deposits.* 34 (5), 999–1015. doi:10.16111/j.0258-7106.2015.05.009

Song, Y., Tang, J., Liu, Z., Li, F., Wang, Q., Xiao, Y., et al. (2019b). Mechanism of Tiegelongnan-Duobuza ramp style ore-controlling structure, Tibet: Evidence from geophysical exploration. *Min. Deposits.* 38 (6), 1263–1277. doi:10.16111/j.0258-7106.2019.06.005

Song, Y., Tang, J., Lu, H., Liu, Z., Li, B., Huang, W., et al. (2022). Discovery of Early Cretaceous skarn Pb-Zn deposit of subduction setting on southern margin of Bangong-Nujiang metallogenic belt and its exploration significance. *Min. Deposits.* 41 (3), 527–542. doi:10.16111/j.0258-7106.2022.03.005

Song, Y., Tang, J., Qu, X., Wang, D., Xin, H., Yang, C., et al. (2014). Progress in the study of mineralization in the Bangongco-Nujiang metallogenic belt and some new recognition. *Adv. Earth Sci.* 29 (7), 795–809. doi:10.11867/j.issn.1001-8166.2014.07.0795

Song, Y., Yang, C., Wei, S., Yang, H., Fang, X., and Lu, H. (2018). Tectonic control, reconstruction and preservation of the tiegelongnan porphyry and epithermal overprinting Cu (Au) deposit, central Tibet, China. *China. Miner.* 8 (9), 398. doi:10.3390/min8090398

Song, Y., Yang, H., Lin, B., Liu, Z., Wang, Q., Gao, K., et al. (2017). The preservation system of epithermal deposits in South Qiangtang terrane of central Tibetan Plateau and its significance: A case study of the tiegelongnan superlarge deposit. *Acta Geosci. Sin.* 38 (05), 659–669. doi:10.3975/cagsb.2017.05.07

Song, Y., Zeng, Q., Liu, H., Liu, Z., Li, H., and Dexi, Y. (2019a). An innovative perspective for the evolution of Bangong-Nujiang ocean: Also discussing the Paleo- and Neo-Tethys conversion. *Acta Petrol. Sin.* 35 (3), 625–641. doi:10.18654/1000-0569/2019.03.02

Sun, J., Mao, J., Beaudoin, G., Duan, X., Yao, F., Ouyang, H., et al. (2017). Geochronology and geochemistry of porphyritic intrusions in the Duolong porphyry and epithermal Cu-Au district, central Tibet: Implications for the Genesis and exploration of porphyry copper deposits. *Ore Geol. Rev.* 80, 1004–1019. doi:10.1016/j.oregeorev.2016.08.029

Sun, X., Bi, Z., Li, G., Zhang, J., and Li, Z. (2015). Regulation of endothelial cell metabolism: Just go with the flow. *Geol. Surv. Chin.* 2, 13–15. doi:10.1161/ATVBAHA.114.304869

Tang, J., Song, Y., Wang, Q., Lin, B., Yang, C., Yang, H., et al. (2016). Geological characteristics and exploration model of the tiegelongnan Cu (Au-Ag) deposit: The first ten million tons metal resources of a porphyry-epithermal deposit in Tibet. *Acta Geosci. Sin.* 37 (6), 663–690. doi:10.3975/cagsb.2016.06.03

Tang, J., Sun, X., Ding, S., Wang, Q., Wang, Y., Yang, C., et al. (2014b). Discovery of the epithermal deposit of Cu (Au-Ag) in the Duolong ore concentrating area, Tibet. *Acta Geosci. Sin.* 35 (1), 6–10.

Tang, J., Wang, Q., Yang, C., Ding, S., Lang, X., Liu, H., et al. (2014a). Two porphyry-epithermal deposit metallogenic subseries in Tibetan Plateau: Practice of "absence prospecting" deposit metallogenic series. *Min. Deposits.* 33 (06), 1151–1170. doi:10.16111/j.0258-7106.2014.06.002

Tang, J., Wang, Q., Yang, H., Gao, X., Zhang, Z., and Zou, B. (2017). Mineralization, exploration and resource potential of porphyry-skarn-epithermal copper polymetallic deposits in Tibet. *Acta Geosci. Sin.* 38 (5), 571–613. doi:10.3975/cagsb.2017.05.02

Tang, X., and Tao, X. (2009). Sedimentary characteristics and tectonic implications of the jingzhushan formation in the coqen region, xizang. *Sediment. Geol. Tethyan Geol.* 29 (1), 53–57.

Wang, B., Wang, L., Chung, S., Chen, J., Yin, F., Liu, H., et al. (2016a). Evolution of the Bangong–Nujiang Tethyan ocean: Insights from the geochronology and geochemistry of mafic rocks within ophiolites. *Lithos* 245, 18–33. doi:10.1016/j.lithos.2015.07.016

Wang, B., Xu, J., Liu, B., Chen, J., Wang, L., Guo, L., et al. (2013). Geochronology and ore-forming geological background of~90Ma porphyry copper deposit in the Lhasa terrane, Tibet plateau. *Acta Geol. Sin.* 87 (1), 71–80.

Wang, D., Tang, J., Ying, L., Chen, X., Xu, J., Zhang, J., et al. (2010). Application of "Five levels+basement" model for prospecting deposits into depth. *J. Jilin Univ. Earth Sci. Ed.* 40, 733–751.

Wang, D., Zhao, Y., Cui, Y., Lu, L., and Xu, H. (2012a). LA-ICP-MS zircon U-Pb dating of important skarn type iron (copper) polymetallic deposits in Baingoin County of Tibet and geochemical characteristics of granites. *Geol. Bull. China.* 31 (9), 1435–1450. doi:10.1007/s11783-011-0280-z

Wang, D., Zhou, B., Zhang, C., and Cheng, L. (2012b). Analysis on geological characteristics and prospecting marks of Baobude lead mine, Tibet. *Chin. J. Geotech. Eng.* 03 (4), 435–440. doi:10.3969/j.issn.1674-7801.2012.04.005

Wang, B., Fang, Y., Wang, Y., Li, S., Gao, Y., Wang, P., et al. (2016b). Catalytic asymmetric ring-opening reactions of aziridines with 3-aryl-oxindoles. *Acta Geosci. Sin.* 37, 691–695. doi:10.1002/asia.201501369

Wang, L., Sun, F., Wang, L., Wang, L., and Zhang, Z. (2018b). Precise design and synthesis of an AIE fluorophore with near-infrared emission for cellular bioimaging. *Glob. Geol.* 37 (2), 399–406. doi:10.1016/j.msec.2018.08.012

Wang, L., Tang, J., Song, Y., Lin, B., and Wang, Q. (2018c). The first discovery of colusite in the tiegelongnan supper-large Cu (Au, Ag) deposit and significance for the genesis of the deposit. *Acta Geol. sin-engl.* 92 (1), 400–401. doi:10.1111/1755-6724.13516

Wang, L., Wang, Y., Danzhen, W., Li, B., Li, Z., Li, S., et al. (2017a). A tentative discussion on metallogeny of the main magmatic-hydrothermal ore deposits in the western Bangong Co-Nujiang metallogenic belt, Tibet. *Acta Geosci. Sin.* 38 (5), 615–626. doi:10.3975/cagsb.2017.05.03

Wang, L., Wang, Y., Fan, Y., and Danzhen, W. (2018a). A Miocene tungsten mineralization and its implications in the Western Bangong-Nujiang metallogenic belt: Constraints from U-Pb, Ar-Ar, and Re-Os geochronology of the Jiaoxi tungsten deposit, Tibet, China. *Ore Geol. Rev.* 97, 74–87. doi:10.1016/j.oregeorev.2018.05.006

Wang, L., Zhao, Y., Wang, A., Li, Y., Li, X., and Guo, S. (2017b). The study of facieology mineragraphy, fluid inclusions, and geochemical characteristics and mineralization in Nadun Cu (Au) deposit, Tibet. *Acta Geol. Sin.* 91 (7), 1565–1588. doi:10.19762/j.cnki.dizhixuebao.2017.07.010

Wang, R., Richards, J., Zhou, L., Hou, Z., Stern, R., Creaser, R., et al. (2015). The role of Indian and Tibetan lithosphere in spatial distribution of Cenozoic magmatism and porphyry Cu–Mo deposits in the Gangdese belt, southern Tibet. *Earth-Science Rev.* 150, 68–94. doi:10.1016/j.earscirev.2015.07.003

Wang, Y., Ma, X., Chen, W., Qu, X., Song, Y., and Tang, J. (2019b). Geochemical characteristics of early cretaceous Cu-rich rocks in middle segment of bangong-nujiang metallogenic belt: A case study of Xiongmei area. *Min. Deposits.* 38 (01), 184–199. doi:10.16111/j.0258-7106.2019.01.013

Wang, Y., Ma, X., Qu, X., and Chen, W. (2019c). Geochronology and petrogenesis of the Xiongmei Cu-bearing granodiorite porphyry in North Lhasa subterrane, central Tibet: Implication for the evolution of Bangong-Nujiang metallogenic belt. *Ore Geol. Rev.* 114, 103119. doi:10.1016/j.oregeorev.2019.103119

Wang, Y., Tang, J., Song, Y., Li, H., Wang, J., Zhang, K., et al. (2019d). Nuclear TAZ activity distinctly associates with subtypes of non-small cell lung cancer. *Bull. Mineral. Petrol. Geochem.* 38 (4), 828–832. doi:10.1016/j.bbrc.2019.01.012

Wang, Y., Tang, J., Wang, L., Li, S., Danzhen, W., Li, Z., et al. (2019a). Magmatism and metallogenic mechanism of the Ga'erqiong and Galale Cu-Au deposits in the west central Lhasa subterrane, Tibet: Constraints from geochronology, geochemistry, and Sr-Nd-Pb-Hf isotopes. *Ore Geol. Rev.* 105, 616–635. doi:10.1016/j.oregeorev.2019.01.015

Wang, Y., Wang, L., Fan, Y., Li, S., Danzhen, W., Zhen, S., et al. (2019e). Geological and geochemical characteristics of the Jiaoxi deposit in the Western Bangong-Nujiang metallogenic belt, Tibet. *Acta Petrol. Sin.* 35 (3), 724–736. doi:10.18654/1000-0569/2019.03.07

Wang, Z., Wang, K., and Yu, W. (2006a). Re-Os isotopic ages of tungsten-molybdenum (bismuth) poly-metallic orede-posit in the Jiagang snowy mountain, Shenzha County, Tibet and theim plication. *Geol. Anhui* 16 (2), 112–116.

Wang, Z., Wu, X., and Wang, K. (2006b). Geochemical characteristics of the garuo monzogranite in the Jiagang xueshan W-Mo(-Bi) district, southwestem xainza, Tibet, China. *Geol. Bull. China.* 25 (12), 1487–1491. doi:10.1111/j.1745-4557.2006.00081.x

Wei, S., Song, Y., Tang, J., Gao, K., Feng, J., Li, Y., et al. (2016). Assembly and analysis of the complete *Salix purpurea* L. (Salicaceae) mitochondrial genome sequence. *Geol. China.* 43 (6), 1894–1912. doi:10.1186/s40064-016-3521-6

Xiao, W., Liu, H., Li, G., Huang, H., Ma, D., Zhang, Z., et al. (2017). Low to moderate temperature, low salinity and enrichment of CO2 hydrothermal fluid at Shangxu orogenic gold deposit in shuanghu, northern xizang (Tibet): Evidence from fluid inclusions, H-O isotopic composition. *Geol. Rev.* 63 (3), 793–808. doi:10.16509/j.georeview.2017.03.018

Xu, J., Zeng, Z., Wang, D., Chen, X., Liu, S., Wang, C., et al. (2008). Nonmuscle myosin light-chain kinase mediates neutrophil transmigration in sepsis-induced lung inflammation by activating beta2 integrins. *Acta Geol. Sin. Chin. Ed.).* 82, 880–886. doi:10.1038/ni.1628

Xu, P., Zheng, Y., Fu, Q., Yang, Z., Shen, Y., Ma, R., et al. (2017). Geology of the Jiagangxueshan W-Mo polymetallic deposit-the first greisen-type W deposit in Tibet. *Acta Petrol. Mineral.* 36 (2), 227–240. doi:10.3969/j.issn.1000-6524.2017.02.008

Xu, P., Zheng, Y., Yang, Z., Hou, Z., Shen, Y., Wang, Z., et al. (2020). Metallogeny of the continental collision-related Jiagang W-Mo deposit, Tibet: Evidence from geochronology and petrogenesis. *Ore Geol. Rev.* 122, 103519. doi:10.1016/j.oregeorev.2020.103519

Yang, C., Beaudoin, G., Tang, J. X., Song, Y., and Zhang, Z. (2020c). Hydrothermal fluid evolution at the Tiegelongnan porphyry-epithermal Cu (Au) deposit, Tibet, China: Constraints from H and O stable isotope and *in-situ* S isotope. *Ore Geol. Rev.* 125, 103694. doi:10.1016/j.oregeorev.2020.103694

Yang, C., Song, Y., Tang, J., Wang, Q., Gao, K., and Wei, S. (2020b). Low temperature history of the Tiegelongnan porphyry-epithermal Cu (Au) deposit in the Duolong ore district of northwest Tibet, China. *Resour. Geol.* 70 (2), 111–124. doi:10.1111/rge.12221

Yang, C., Tang, J., Beaudoin, G., Song, Y., Lin, B., Wang, Q., et al. (2020a). Geology and geochronology of the Tiegelongnan porphyry-epithermal Cu (Au) deposit, Tibet, China: Formation, exhumation and preservation history. *Ore Geol. Rev.* 123, 103575. doi:10.1016/j.oregeorev.2020.103575

Yang, C., Tang, J., Wang, Y., Yang, H., Wang, Q., Sun, X., et al. (2014). Fluid and geological characteristics researches of Southern Tiegelong epithemal porphyry Cu-Au deposit in Tibet. *Min. Deposits.* 33 (6), 1287–1305. doi:10.16111/j.0258-7106.2014.06.009

Yang, S., Li, D., Chen, G., Li, H., Zhang, S., and Zhou, T. (2018). The discovery of the Wuluqiong magnetite deposit in Tibet and its geological characteristics. *Geol. China.* 45 (6), 1214–1227. doi:10.12029/gc20180611

Yang, Y., Zhang, Z., and Tang, J. (2015). Mineralization, alteration and vein systems of the Bolong porphyry copper deposit in the Duolong ore concentration area, Tibet. *Geol. China* 42 (3), 759–776.

Yang, Z., Hou, Z., White, N. C., Chang, Z., Li, Z., and Song, Y. (2009). Geology of the post-collisional porphyry copper–molybdenum deposit at Qulong, Tibet. *Ore Geol. Rev.* 36 (1), 133–159. doi:10.1016/j.oregeorev.2009.03.003

Yin, A., and Harrison, T. M. (2000). Geologic evolution of the Himalayan-Tibetan orogen. *Annu. Rev. Earth Planet. Sci.* 28 (1), 211–280. doi:10.1146/annurev.earth.28.1.211

Yu, H., Chen, J., Xu, J., Wang, B., Wu, J., and Liang, H. (2011a). Geochemistry and origin of late cretaceous (~90Ma) ore-bearing porphyry of Balazha in mid-northern Lhasa terrane, Tibet. *Acta Petrol. Sin.* 27 (7), 2011–2022.

Yu, H., Gao, Y., Yang, Z., Tian, S., Liu, Y., Cao, S., et al. (2011b). Zircon LA-ICP-MS U-Pb dating and geochemistry of intrusive rocks from Gunjiu iron deposit in the Nixiong ore field, Coqen, Tibet. *Acta Petrol. Sin.* 27 (7), 1949–1960. doi:10.1016/j.sedgeo.2011.06.007

Yu, Y., Yang, Z., Liu, Y., Tian, S., Ji, X., Gao, Y., et al. (2012). Mineralogical characteristics and 40Ar-39Ar dating of phlogopite from the gunjiu iron deposit in the Nixiong ore field, coqen, Tibet. *Acta Petrol. Mineral.* 31 (5), 681–690. doi:10.3969/j.issn.1000-6524.2012.05.006

Zeng, Q., Wang, B., Xiluo, L., Mao, G., Liu, H., and Liu, G. (2020). Suture zones in Tibetan and Tethys evolution. *Earth Sci.* 8, 2735–2763. doi:10.3799/dqkx.2020.152

Zeng, Y., Xu, J., Ducea, M. N., Chen, J., Huang, F., and Zhang, L. (2019). Initial rifting of the Lhasa terrane from Gondwana: Insights from the permian (~262 Ma) amphibole-rich lithospheric mantle-derived yawa basanitic intrusions in southern Tibet. *J. Geophys.* 124 (3), 2564–2581. doi:10.1029/2018JB016281

Zhang, R., Wang, Y., Wang, W., Liu, J., and Yuan, L. (2019b). Zircon U-Pb-Hf isotopes and mineral chemistry of Early Cretaceous granodiorite in the Lunggar iron deposit in central Lhasa, Tibet Y, China. *J. Cent. South Univ. Engl. Ed.* 26 (12), 3457–3469. doi:10.1007/s11771-019-4266-5

Zhang, R., Xiong, F., Xu, X., Liu, Z., and Yang, J. (2019a). The feature and tectonic setting of chromitite from the Yilashan ophiolite in Tibet. *Acta Geol. Sin.* 93 (7), 1655–1670. doi:10.19762/j.cnki.dizhixuebao.2019061

Zhang, X., Li, G., Qin, K., Lehmann, B., Li, J., Zhao, J., et al. (2018a). Petrogenesis and tectonic setting of Early Cretaceous granodioritic porphyry from the giant Rongna porphyry Cu deposit, central Tibet. *J. Asian Earth Sci.* 161, 74–92. doi:10.1016/j.jseaes.2018.05.006

Zhang, X., Tang, J., Chen, Y., Yao, X., Song, J., and Li, Z. (2018b). Magma origin of two series of volcanic rocks from gaerqiong-galale Cu-Au ore concentrated area of Tibet and its geological significance: Implication from Hf isotope characteristics. *J. Mineral. Petrol.* 38 (3), 87–95.

Zhang, Y., Shi, G., and Shen, S. (2013). A review of Permian stratigraphy, palaeobiogeography and palaeogeography of the Qinghai–Tibet Plateau. *Gondwana Res.* 24 (1), 55–76. doi:10.1016/j.gr.2012.06.010

Zhang, Z., Fang, X., Tang, J., Wang, Q., Yang, C., Wang, Y., et al. (2017). Chronology, geochemical characteristics of the Gaerqin porphyry copper deposit in the Duolong ore concentration area in Tibet and discussion about the identification of the lithoscaps and the possible epithermal deposit. *Acta Petrol. Sin.* 33 (2), 476–480. doi:10.3760/cma.j.issn.0529-5815.2017.06.016

Zhang, Z., Geng, Q., Peng, Z., Cong, F., and Guan, J. (2011). Geochemistry and geochronology of the Caima granites in the Western part of the Bangong Lake-Nujiang metallogenic zone, Xizang. *Sediment. Geol. Tethyan Geol.* 31, 86–96. doi:10.3969/j.issn.1009-3850.2011.04.013

Zhang, Z., Geng, Q., Peng, Z., Cong, F., and Guan, J. (2015c). Petrogenesis of Fuye pluton in rutog, Tibet: Zircon U-Pb dating and Hf isotopic constraints. *Geol. Bull. China.* 34, 262–268. doi:10.1002/marc.201400489

Zhang, Z., Yao, X., Tang, J., Li, Z., Wang, L., Yang, Y., et al. (2015a). Lithogeochemical, Re-Os and U-Pb geochronological, Hf-Lu and S-Pb isotope data of the Ga'erqiong-galale Cu-Au ore-concentrated area: Evidence for the late cretaceous magmatism and metallogenic event in the bangong-nujiang suture zone, northwestern Tibet. *Resour. Geol.* 65 (2), 76–102. doi:10.1111/rge.12064

Zhang, Z., Zhang, H., An, C., Wang, B., and Liu, X. (2015b). Nut consumption and risk of stroke. *Mineral Resour. Geol.* 29 (2), 189–196. doi:10.1007/s10654-015-9999-3

Zhao, Y., Cui, Y., Lv, L., and Shi, D. (2011). Chronology, geochemical characteristics and the significance of Shesuo copper polymetallic deposit, Tibet. *Acta Petrol. Sin.* 27 (7), 2132–2142.

Zhao, Y., Song, L., Fan, X., Shi, D., Zang, T., Chen, H., et al. (2009). Re-Os dating of molybdenite from the Shesuo copper polymetallic ore in shenzha county Tibet and its geological significance. *Acta Geol. Sin.* 83 (08), 1150–1158. doi:10.3321/j.issn:0001-5717.2009.08.013

Zheng, W., Tang, J., Zhong, K., Ying, L., Leng, Q., Ding, S., et al. (2016). Geology of the Jiama porphyry copper–polymetallic system, Lhasa Region, China. *Ore Geol. Rev.* 74, 151–169. doi:10.1016/j.oregeorev.2015.11.024

Zheng, Y., Ci, Q., Gao, S., Wu, S., Jiang, X., and Chen, X. (2021). The Ag-Sn-Cu polymetallic minerogenetic series and prospecting direction in the Western Gangdese belt, Tibet. *Earth Sci. Front.* 28 (3), 379–402. doi:10.13745/j.esf.sf.2021.1.19

Zhong, Y., Hu, X., Liu, W., Xia, B., Zhang, X., Huang, W., et al. (2018). Age and nature of the jurassic–early cretaceous mafic and ultramafic rocks from the yilashan area, bangong–nujiang suture zone, central Tibet: Implications for petrogenesis and tectonic evolution. *Int. Geol. Rev.* 60 (10), 1244–1266. doi:10.1080/00206814.2017.1385033

Zhou, J., Meng, X., Zang, W., Yang, Z., Xu, Y., and Zhang, X. (2013). Zircon U-Pb geochronology and trace element geochemistry of the ore-bearing porphyry in Qingcaoshan porphyry Cu-Au deposit, Tibet, and its geological significance. *Acta Petrol. Sin.* 29 (11), 3755–3766. doi:10.1021/je00056a024

Zhu, D., Li, S., Cawood, P. A., Wang, Q., Zhao, Z., Liu, S., et al. (2016). Assembly of the Lhasa and Qiangtang terranes in central Tibet by divergent double subduction. *Lithos* 245, 7–17. doi:10.1016/j.lithos.2015.06.023

Zhu, X., Chen, H., Liu, H., Ma, D., Li, G., Huang, H., et al. (2015b). Zircon U-Pb ages, geochemistry of the porphyries from the Duobuza porphyry Cu-Au deposit, Tibet and their metallogenic significance. *Acta Geol. Sin. Chin. Ed.).* 89 (3), 534–548. doi:10.19762/j.cnki.dizhixuebao.2015.03.008

Zhu, X., Chen, H., Liu, H., Ma, D., Li, G., Zhang, H., et al. (2015c). Clinical characteristics of leg restlessness in Parkinson's disease compared with idiopathic Restless Legs Syndrome. *Acta Geol. Sin.* 89 (1), 109–114. doi:10.1016/j.jns.2015.07.008

Zhu, X., Chen, H., Ma, D., Huang, H., Li, G., Li, Y., et al. (2011). Re-Os dating for the molybdenite from Bolong porphyry copper-gold deposit in Tibet, China and its geological significance. *Acta Petrol. Sin.* 27 (7), 2159–2164.

Zhu, X., Chen, H., Ma, D., Huang, H., Li, G., Liu, C., et al. (2012). (40 Ar/(39) Ar dating for K-feldspar from Duobuza porphyry copper-gold deposit in Tibet, China and its geological significance. *Geoscience* 26 (4), 656–662.

Zhu, X., Li, G., Chen, H., Ma, D., and Huang, H. (2015a). Zircon U-Pb, molybdenite Re-Os and K-feldspar 40Ar/39Ar dating of the bolong porphyry Cu-Au deposit, Tibet, China. *Resour. Geol.* 65 (2), 122–135. doi:10.1111/rge.12059